AIR BUBBLES FOR WATER QUALITY IMPROVEMENT

Report No OD/12
April 1978

Hydraulics Research Station
Wallingford
Oxon OX10 8BA
Telephone 0491 35381

ABSTRACT Thermal stratification in water supply reservoirs can result in a serious degradation in water quality. The techniques of artificial mixing and aeration, using air bubbles, have been applied in a number of impoundments to prevent the formation of the anaerobic conditions that lead to poor water quality. The first part of this report describes some of the aeration and mixing devices that have been used, and discusses the parameters used to compare their efficiency. The second part of the report presents measurements on the pumping and mixing performance of a destratification device that uses large (300 mm diameter) air bubbles. Experiments were conducted at laboratory and near-prototype scales. The experimental data is used to develop a design guide for large air bubble guns.

CONTENTS

TABLES

FIGURES

FIGURES (Continued)

INTRODUCTION 1

Increases in population and living standards in developing countries has intensified the demand for water. To satisfy this demand new water supplies are being tapped and serious thought is being given to methods of water conservation. In arid and semi-arid areas, where the availability of water may be the limiting factor in economic development, attention is being focussed on new methods of conserving existing water supplies. In many regions the supply of water can be secured by storing water in times of surplus, for use in times of shortage. Water is usually stored in surface impoundments, although forms of sub-surface storage may become increasingly important. Water in surface impoundments is subject to losses from seepage and evaporation, and if thermal stratification occurs, to a degradation in water quality.

Water temperature in lakes and reservoirs varies seasonally, due to heat exchange between the water surface and the atmosphere. The corresponding water density changes can lead to the formation of density differences between the surface layers and the colder deeper layers near the bottom of an impoundment. The appearance of density differences is often sufficient to prevent mixing and aeration in the lower part of lakes and reservoirs, except that produced by high winds. Water in the lower layers is effectively isolated from the surface zone, and can become rapidly deoxygenated by biological activity. This, in turn, may lead to a severe deterioration in water quality.

A number of devices, many utilising compressed air, have been used to artificially mix and aerate stratified impoundments to improve the quality of the stored water. It has been suggested that artificial destratification may also lead to a reduction in evaporative water losses. The first part of this report, a literature review, includes a brief description on the processes that lead to poor water quality and a description and comparison of the devices used to increase dissolved oxygen levels in stratified impoundments. The effect of artificial destratification on evaporation rates is also discussed. The second part of the report describes measurements of the efficiency of destratification and the mixing processes produced by large air bubbles formed in devices similar to the "Aero-Hydraulics Gun". Bubbles ranging in size between 0.03 m and 0.3 m were used and the results obtained form the basis of a design method for large bubble guns.

PART I

LITERATURE REVIEW 2

Thermal stratification and water quality

The effects that lead to thermal stratification, and the resulting consequences on water quality are complex. The simple outline account given here follows that given by Collingwood (Ref 1).

Thermal stratification 2.1

A stratified impoundment usually consists of three layers, described by a characteristic vertical temperature and dissolved oxygen distribution. The upper layer, or epilimnion, is usually mixed and aerated by wind action. The transition layer, or thermocline, is characterised by a large temperature (density) gradient. The lower layer, or hypolimnion, contains the coldest water and has a low dissolved oxygen content (see Fig 1).

Season, climate, impoundment size and shape, exposure to wind, and the magnitude of inflows and outflows can all affect the thickness of the epilimnion. The epilimnion thickness is usually in the range 5 to 10 m, but can be much deeper in large impoundments. The thermocline (Fig 1), can be defined as the region in which the temperature variation is larger than one degree centigrade/metre. It has been suggested, (Ref 2), that for Japanese impoundments the thermocline thickness is proportional to the square root of reservoir surface area.

The degree of stratification varies seasonally, following the temporal variation in solar radiation. Stratification is strongest at the end of the summer period and decays in the autumn as air temperatures reduce. Solar radiation is absorbed exponentially with depth, heat being transported downwards to the thermocline by wind induced turbulent mixing. Vertical mixing is suppressed by the density gradient at the thermocline, but strong winds can result in turbulent erosion and also tilting of the thermocline (Ref 1). Winds can produce a natural destratification in reservoirs when density differences are small.

Water quality in a stratified impoundment 2.2

Planktonic algae require both light and nutrients, and are usually confined to the epilimnion (Fig 1). Algae and other organic material from reservoir inflows fall to, and cover the reservoir floor, creating an oxygen demand as decomposition occurs. In new impoundments decomposition of organic material not cleared before flooding can also create a large additional oxygen demand (Ref 3).

Oxygen demand in the hypolimnion is met by surface aeration and photosynthesis. The hypolimnion, too deep for light to penetrate, is isolated from the surface layer and has only a limited dissolved oxygen store. As this is depleted by biological activity, chemical reactions occur which release inorganic materials, affecting the taste and colour of impounded water and leading to high water treatment costs. Other reported problems include the formation of algael blooms, corrosion, and fish mortality within stratified impoundments and in discharged downstream waters (Refs 1,4,30). Cold deoxygenated water may also have adverse effects on crops irrigated with water discharged from the hypolimnion of stratified impoundments (Ref 2).

The effects of stratification on water quality are most severe in reservoirs impounding polluted or high organic content water. Oxygen depletion can, however, occur in the hypolimnion of reservoirs impounding unpolluted or low organic content water (Ref 4).

A number of biological, chemical, and engineering techniques have been developed to alleviate water quality problems in storage impoundments (Ref 3). Methods that have been applied to stratified impoundments,

artificial destratification and hypolimnion aeration, are discussed in the following sections.

ARTIFICIAL DESTRATIFICATION 3

The objective of artificial destratification is to improve water quality by increasing dissolved oxygen levels, and thus reducing the concentration of organic and inorganic materials in solution. Aeration is achieved by transferring hypolimnion water across the thermocline and mixing it in the epilimnion. A number of techniques, including air lift devices, pumped water jets, and mechanical pumps have been used. Oxygenation occurs from natural surface aeration, photosynthesis, and by oxygen transfer from the rising air bubbles when air bubble mixing is used. The thermocline is moved downwards by the pumping action of the mixing device and by erosion from the turbulent motion induced in the upper layer. Eventually complete destratification occurs.

Artificial destratification has, in general, been successfully applied as a technique for water quality improvement (Ref 5). However, the reported effects on the formation of algael blooms are contradictory, and some of the other consequences of artificial mixing may not be desirable. This will be discussed in section 4.

Methods for artificial destratification 3.1

Some of the methods that have been used to achieve artificial destratification are shown in Fig 2, and are described below.

Mechanical pumps 3.1.1

Conventional pumps have been used to direct water jets from the base of an impoundment to promote circulation and mixing. This technique has been used successfully in the Thames Valley reservoirs in the UK (Refs 25,26). Systems of this type can be installed as a permanent device during the construction stage of an impoundment, and are usually applied to pumped storage schemes.

In a technique more suited to existing reservoirs a pump mounted on a raft is moored over the deepest section of an impoundment and water is pumped from the hypolimnion via a vertical pipe and discharged near the water surface (Fig 2a), (Ref 5). An alternative technique in which epilimnion water is pumped to the hypolimnion has also been suggested (Refs 6,7).

Compressed air mixing 3.1.2

Compressed air has been used to achieve destratification in many installations. Small air bubbles, ranging in diameter between 4 mm and 20 mm are released at the base of an impoundment from a group of diffusers (Fig 2b), or over a larger area from a long perforated pipe (Fig 2c). The rising air bubbles produce a buoyant jet flow, which entrains water from the hypolimnion and epilimnion and induces mixing in the impoundment. The turbulent jet can also lead to the formation of a secondary circulating flow pattern in the epilimnion. Typical installations of this type are described in Refs 2,8,9,10,11.

A number of mixing devices using compressed air are commercially available. All the available systems are not mentioned below, and the description of particular devices does not indicate the merit of one system over another.

Bubble screens have been installed by the Hinde Corporation (Air Aqua) in North America, (Fig 2b), (Refs 12,13). Bubbles ranging in diameter between 0.4 mm and 4 mm are released from "check valves" contained in lengths of weighted polythene pipe. Atlas Copco have installed bubble screen devices for artificial destratification, and other applications including salinity barriers, and barriers to contain oil spills in harbours (Refs 14,15,16).

The "Helixer", (Fig 2d), manufactured by the Polycon Corporation, has been installed in a number of impoundments. It consists of a 0.46 m diameter polythene tube containing a vertically aligned spiral. Air bubbles released at the base of the "Helixer" induce water flow in a spiral path through the device. It is claimed that the large shear forces developed within the "Helixer" result in a high oxygen transfer rate (Refs 18,19 20).

The "Aero-Hydraulics Gun" (Fig 2e) uses large, 0.3 m diameter, bubbles to pump water from the hypolimnion to the upper layer in a vertically aligned pipe. Bryan (Ref 21) describes applications in a number of impoundments. Measurements of the efficiency of a similar device forms Part II of this report.

Ref 22 contains information on capital and operating costs for a variety of mixing methods.

Oxygen transfer 3.2 When mechanical pumps are used for destratification surface aeration is the primary mechanism for oxygen transfer, although photosynthesis may also be significant (Ref 3). Neilson, (Ref 23), has investigated the contribution to the total oxygen transfer rate of oxygen transfer from rising air bubbles when small bubble mixing devices are used. Neilson calculated the oxygen transfer rates from rising air bubbles in a hypothetical impoundment 10 m deep and 150 m wide. Oxygen transfer rates for the bubble formation, rise, and at the surface boil were derived from the results obtained in a laboratory experiment using 5 mm diameter bubbles in an open and closed tank. When compared with surface aeration the contribution from the air bubbles was small, (6% to 12%) depending on the values chosen to represent natural surface aeration. Neilson concluded that small bubble destratification systems should be designed to maximise mixing efficiency and to promote circulation in the impoundment.

This conclusion is in agreement with field data obtained in shallow to medium depth impoundments. For example, Tolland (Ref 11) measured dissolved oxygen concentrations perpendicular to the axis of a bubble screen installation in an impoundment 14.5 m deep and concluded that surface aeration is the dominating mechanism for the reaeration process. Symons (Ref 9) could detect no change in the oxygen content of bubbles rising in an impoundment 19 m deep.

An increase in hydrostatic pressure, which is the case with deep impoundments, will increase the rate of oxygen transfer from rising air bubbles to the impounded water. This effect was noted by Bernhardt, (Ref 8), in a destratification experiment in which 10 mm to 20 mm diameter bubbles were released from a nozzle at the base of a deep (43 m) impoundment. The oxygen content of the rising bubbles was reduced by 24% during the bubble rise, indicating significant oxygen transfer. Most of the oxygen transfer occurred during the first 19 m of the bubble rise, the change between a depth of 18 m and the free surface being negligibly small. It can be, therefore, concluded that oxygen transfer from rising air bubbles will become important in deep impoundments.

Thermocline movement 3.3 The thermocline is depressed as water is transferred from the hypolimnion and mixed in the epilimnion by the pumping action of the mixing device, and also by turbulent erosion induced in the upper layer. In an investigation conducted by Symons, (Refs 6,24), water was pumped from the hypolimnion through a pipe and discharged in the upper layers. Destratification was completed after only 50% of the initial hypolimnion volume had been pumped. It was concluded that a large part of the downward

movement of thermocline was due to turbulence generated by the discharged jet. Turbulence generated by wind will also promote vertical mixing and hence erosion and downward movement of the thermocline (Ref 25). The contribution of turbulent erosion to the total rate of thermocline movement will depend on a number of factors. In a particular impoundment the magnitude of turbulent erosion will be determined by the strength of the density stratification, the action of the mixing device, and the effects of wind.

Efficiency comparisons 3.4

Although a number of studies concerned with the effects of artificial destratification on water quality have been reported, an assessment of the hydraulic efficiency of the used mixing device has been made in relatively few cases.

Symons (Refs 5,9,24,27), compared the performance of mechanically pumped and small air bubble destratification devices. The parameters used to compare the performance of the two systems were destratification efficiency and oxygenation efficiency. Knoppert, (Ref 10), has suggested that the volume of water pumped per unit volume of air supplied provides an alternative comparative parameter for air bubble destratification systems.

Destratification efficiency 3.4.1

The efficiency of a destratification device can be defined as the change of impoundment potential energy (stability) per unit power input to the mixing device. Stability can be calculated as the work required to lift the total water mass the distance between the mass centre of gravity when an impoundment is stratified and the mass centre of gravity when the impoundment is fully mixed. This represents the theoretical work required to mix a stratified impoundment.

In practice, the factors listed below complicate the use of destratification efficiency as a comparative parameter. Results obtained under field conditions must be interpreted with extreme caution, particularly when experiments conducted in different impoundments using different mixing devices are being compared.

a) Stability often follows a seasonal cycle, reflecting the temporal variation in climate. Short-term fluctuations, caused for example by strong winds or periods of hot calm weather are superimposed on the seasonal pattern. These natural variations will be included in the change in impoundment stability measured during artificial mixing, and can have a large influence on a destratification efficiency calculated for a mixing device. Symons (Ref 9), discusses methods of correcting measured stability changes to account for natural variations, but these methods can, at best, only be approximate.

b) The static pressure head difference associated with density differences, that occur in a stratified reservoir, will usually be very small in comparison with the head losses generated in a mixing device. Thus the discharge from, for example a mechanical pump, or as shown later from a "large bubble gun", is virtually unaffected by seasonally changing water density differences. Hence, measured destratification efficiencies can depend strongly on the degree of stratification at the time of mixing.

c) Stability time curves obtained during artificial mixing show an approximately exponential decay in stability as mixing proceeds (Ref 9,10,28). The shape of these curves indicates that a larger destratification efficiency will be obtained for a partial mixing than for a complete mixing. In practice, mixing is often continued until the required water quality conditions are achieved. This makes it difficult to compare results from experiments in which measurement of the hydraulic efficiency of the mixing device was not the primary objective,

as the destratification efficiency obtained will depend on the point at which mixing was stopped.

d) As the power input to the mixing device is used to calculate destratification efficiency the mechanical efficiency of the used pump or air compressor can affect the result. This can distort the comparison between different mixing methods, as the devices used may not have been operated at their maximum mechanical efficiency.

The variations that can occur in measured destratification efficiencies, even after corrections have been applied to account for natural stability changes, are illustrated in the data reported in Ref 9. When a small bubble mixing device was used to destratify an impoundment a number of times during one season, corrected destratification efficiencies varied between 0.6% and 1.5%.

Oxygenation efficiency 3.4.2

This is defined as the mass of oxygen transferred to water, per unit power input to the mixing device. As the objective of artificial destratification has been to increase dissolved oxygen levels this would appear to be a more relevant comparative parameter. However, the primary mechanism for oxygen transfer will usually be surface aeration. This is controlled, as mentioned previously, principally by local wind conditions, and the volume and oxygen content of hypolimnion water brought to the surface zone. When all other conditions are the same a larger mass of oxygen will be transferred when hypolimnion dissolved oxygen levels are low, or when an oxygen demand exists, than when initial dissolved oxygen levels are close to saturation (see Ref 9). Of the factors mentioned above only the volume of hypolimnion water pumped to the surface zone is a property of the mixing device. Measured oxygenation efficiencies can thus depend to a large extent on the water quality and the wind conditions at the time of measurement.

Pumping efficiency 3.4.3

The pumping efficiency of air bubble mixing devices is defined as the volume of hypolimnion water transferred across the thermocline, per unit volume of compressed air supplied. Knoppert, (Ref 10), suggests that this provides a better comparative performance parameter than destratification efficiency, as variations in climate will have a smaller effect on the volume of hypolimnion water pumped across the thermocline than on stability changes (see section 3.4.1). Unfortunately the only experimental data available for the case of a temperature stratified reservoir is that presented by Knoppert, and a classification of other workers' results on this basis is not possible from the limited information in the literature.

Destratification systems – comparative performance data 3.4.4

Table 1 shows measured data obtained from a number of destratification experiments. For the reasons given in the previous sections these results can only be used to give a very approximate indication of likely performance. Some information can, however, be gained from experiments where different destratification systems have been evaluated in the same impoundment.

Mechanical pumping, small air bubble devices 3.4.5

The data in Table 1 shows that mechanically pumped destratification devices appear to have been less efficient than mixing devices using small air bubbles. The performance of both systems has been compared in the same impoundment by Symons (Refs 5,9,24,27). Bearing in mind the qualifications outlined in the previous sections, larger destratification and oxygenation efficiencies were obtained with the air bubble system. The larger oxygenation efficiency produced by the small air bubble system

was attributed to the larger volumes of hypolimnion water pumped to the surface zone, as oxygen transfer from the rising bubbles was negligibly small. This comparison is questionable because of the low hydraulic efficiency of the pumping system used (see Refs 6,9,29). Quintero (Ref 7) outlines the design of a higher efficiency mechanically pumped device with applications (one only partially successful) being described in Refs 30 and 31. It appears that air bubble systems may be more efficient than mechanical pumps, although the advantage may not be as clear cut as suggested by the data in Table 1. However, practical considerations will often make the use of small air bubble systems attractive for use in existing impoundments. The air compressor is shore based, which minimises problems of power supply and maintenance, and no floating structure is required. A bubble screen device is simple and cheap to manufacture, and can be rapidly installed from a small boat (see for example Ref 18).

Comparison of small bubble mixing methods 3.4.6

Knoppert, (Ref 10), has compared the mixing performance of small air bubbles released from a single diffuser with that of a bubble screen produced by a large perforated pipe. Equal destratification efficiencies were obtained (Table 1). It was concluded that the bubble screen was more efficient than the single diffuser by comparing the pumping efficiencies produced by both devices. It is noted that the bubble screen experiment was conducted in the summer, when natural stability was probably increasing, and that the single diffuser experiment was conducted in the autumn, when natural stability was probably decreasing. Knoppert did not attempt to correct his results to account for the natural stability changes.

Kobus, and Cederwall and Ditmars, (Refs 32,33), have presented equations predicting the water volume flux induced when air bubbles are released from line and point sources. These can be used to predict the gross behaviour of air bubble plumes in a homogeneous ambient fluid. However, the presence of a density stratification precludes the use of these analyses for the prediction of destratification performance. At and above the density interface the relative buoyancy between the air bubble/water plume and the ambient fluid is reduced. This may result in some or all of the pumped hypolimnion water "peeling off" from the plume and sinking back to the hypolimnion. (This mechanism is called "uncoupling" by Cederwall.) The effects of turbulent thermocline erosion are not included in the analysis of air bubble plumes derived for the case of a homogeneous ambient fluid.

However, the analytical expressions in Refs 32,33 and laboratory scale experimental results presented by Kobus and Knoppert (Refs 32,10) show that the largest isothermal pumping efficiencies are obtained with a low air volume flux loadings at the diffuser. In a practical installation this is most easily achieved with a long perforated pipe producing small bubbles. Cederwall concludes that this will be the most efficient design for a small air bubble mixing device.

"Large bubble guns" 3.4.7

Symons (Refs 9, 34) has presented data on the destratification efficiency of an "Aero-Hydraulics Gun" (see Table 1). Although the destratification efficiency was less than has been obtained with some of the small bubble systems the validity of a comparison based on destratification efficiencies is doubtful (see Ref 9 and the comments in section 3.4.1). In spite of the apparent success of this installation the six bubble guns were subsequently replaced with a single commercially available small bubble mixing and aeration device (Ref 35).

Experiments described later in this report showed that a simple small bubble mixing device produced much larger pumping efficiencies than a "large-bubble gun". This result should be accepted with reserve as the

test conditions did not fully represent a reservoir situation.

HYPOLIMNION AERATION 4

The effects of artificial destratification may be undesirable in some impoundments. Thermal mixing increases water temperatures below the original thermocline position, and this may be unacceptable if abstracted water is used for water cooling or public supply (Ref 8). Destratification, although possibly beneficial for some fish populations (Ref 30), may have adverse effects on species requiring the cold water habitat found in the hypolimnion (Refs 36,37).

Hypolimnion aeration devices have been developed to increase dissolved oxygen levels in the hypolimnion, without causing destratification. Fast (Ref 38) lists seventeen proposed hypolimnion aeration devices, twelve of which have been tested in the field. These can be divided into three groups, mechanical agitation and pumping, pure oxygen injection, and full and partial air lift devices using compressed air. Fast (Ref 37) has also estimated capital and running costs for the three systems which appear to be most promising, and for which performance data is available. Technical data from this and other sources is shown in Table 2. The techniques involving pure oxygen injection have been described by Speece (Ref 39) and Fast (Ref 40). These may not find many applications in developing countries as large quantities of liquid oxygen are required.

Full and partial air-lift hypolimnion aerators are shown in Fig 3. In the full air-lift device, first described by Bernhardt (Ref 8) and later improved (Ref 41), water from the hypolimnion is lifted and aerated by air bubbles released at the base of a vertical pipe. At the surface the air bubbles are vented to the atmosphere and the cold dense hypolimnion water is returned to the base of the impoundment. In the Limno, (Atlas, Copco), aeration occurs in a chamber anchored at the base of the hypolimnion. A full description and results of oxygen transfer measurements in an impoundment are given in Ref 36. It is noted that high dissolved nitrogen concentrations, which may be toxic to fish, were produced by the Limno.

The largest oxygenation efficiencies have been obtained with the full air-lift hypolimnion aerator described by Bernhardt (Refs 8,41) in which 50% of the oxygen supplied was transferred to the hypolimnion. Fast (Ref 37) concludes that the lowest capital and operating costs will be achieved with this form of hypolimnion aerator.

ARTIFICIAL DESTRATIFICATION FOR EVAPORATION CONTROL 5

Artificial destratification can reduce the temperature of the surface layers in a lake or reservoir, this in turn may reduce evaporative water losses. Artificial mixing resulted in a net reduction in evaporation of about 5% at Lake Woolford (Ref 28) and between 4% to 10% El Capitan reservoir (Ref 42).

Hughes (Ref 43) has used a mathematical model to predict the reduction in evaporation, following artificial destratification, for deep impoundments in Utah, USA. Experiments with cooled and stirred Class A evaporation pans were used to confirm, for a very small water surface, the expression used to relate percentage evaporation suppression to a reduction in water surface temperature. Hughes' results indicate that the magnitude of evaporation suppression depends principally on the volume of hypolimnion water available for mixing, and sufficient outflow to abstract the heat gain

resulting from a reduction in evaporation. The reservoir outflow must be below the position of the natural thermocline, before the reservoir is artificially mixed, to achieve a reduction in evaporation on an annual basis.

Table 3 shows the correlation obtained between evaporation suppression, impoundment maximum depth, and flow index, when the analysis was applied to ten Utah impoundments. It should be noted that this data will only apply for climatic conditions similar to those in Utah. In his calculation Hughes makes few assumptions. Noted that the equation used to predict evaporation suppression is valid when applied to a large reservoir. In fact the equation used is sensitive to changes in air temperature and relative humidity in the downwind direction and its use for a large water surface remains to be confirmed experimentally.

SUMMARY AND CONCLUSIONS 6

A number of techniques including mechanical and diffused air pumping have been used to achieve artificial destratification in water storage impoundments. These methods have usually been successful in improving the quality of the stored water. Although accurate comparisons of the efficiency of the various available destratification devices cannot be made it appears that the largest operating efficiencies have been achieved with small air bubble devices. Small air bubble devices can also offer practical advantages for installations in existing impoundments.

Aeration usually occurs through the free surface, except in deep impoundments where oxygen transfer from rising air bubbles may be significant.

Hypolimnion aeration devices have been developed to increase hypolimnion dissolved oxygen levels in cases where artificial destratification would not be acceptable. Oxygenation efficiencies are usually lower for hypolimnion aeration than for artificial mixing.

It has been suggested that artificial destratification will result in a substantial reduction evaporative water losses in deep impoundments. This must be accepted with reserve and further theoretical and experimental work is necessary to determine the effectiveness of this technique as a method of evaporation control.

PART II

LARGE AIR BUBBLES EXPERIMENT

INTRODUCTION 7

The literature review has shown that air bubble mixing devices have been successfully used for reservoir destratification. In many installations small air bubbles were released from a diffuser placed at the base of an impoundment. Alternatively large air bubbles can be used for destratification purposes. An experiment was therefore conducted to determine the efficiency of a device, producing large air bubbles. The device was similar to that of "Aero-Hydraulics Gun" as described by Bryan (Ref 21), and the efficiency of the device was determined when it was operating under various laboratory conditions.

The bubble gun used in the experiments operates as a low head, high volume displacement pump. Compressed air enters the base of the bubble production device (see Fig 4) at chamber A, displacing water from chambers A and B until the water level reaches the bottom of the central pipe C. Air accumulated in chambers A and B then escapes via the pipe C, forming a large air bubble at the base of the stack pipe S. The air bubble, of diameter D, then rises up the stack pipe acting as a piston, causing water to be drawn in at the water inlet port of gap size G (see Fig 4). The bubble release frequency depends on the compressed air supply Q_a, the diameter of chambers A and B, and the length and diameter of the pipe C. Large air bubbles are released intermittently, and produce a continuous pulsating flow in the stack pipe.

When used for artificial destratification a group of bubble guns is usually anchored at the deepest section of an impoundment, with the top of the stack pipes positioned at, or just above, the natural thermocline (Ref 21). The turbulent jet of pumped hypolimnion water emerging from the stack pipe entrains epilimnion water, and causes turbulent motion and mixing in the epilimnion. This may in turn result in turbulent erosion of the thermocline.

In assessing the performance of bubble guns the distinction should be made between pumping efficiency, and efficiency of destratification. The volume of water discharged from the top of the stack pipe will depend principally on the gun dimensions, the air bubble release frequency, and the depth from which air bubbles are released. Providing the flow into the water inlet port (see Fig 4) is not restricted by the tank walls, the pumping performance will not be affected by the size of the tank in which the measurements are made. When assessing the destratification performance of the device the following additional factors need to be considered:—

a) The influence of the test tank size and the location of the gun on the mixing process.

b) The depth and temperature elevation of the warm surface layer used to represent the epilimnion.

A series of experiments have been conducted in two laboratory tanks with model guns having diameters D = 25 mm, 75 mm and 144 mm. Cold and warm water layers were used to represent a stratified impoundment. Further experiments were made to evaluate the pumping performance of guns with dimensions closer to the prototype scale; in order to minimise scale effect, and to obtain results at large values of stack pipe length to diameter ratio. These experiments were conducted in a 15 m x 15 m x 10 m deep tank. A number of mixing experiments with temperature stratified layers were also made. Details of all the tank and gun dimensions used for these experiments are shown in Table 4.

FLOW VISUALISATION 8

A preliminary experiment was carried out in a small transparent tank, 0.76 m x 0.76 m x 0.45 m deep, to study the mixing process produced by a model gun of stack diameter D = 25 mm. Cold and warm water layers with an initial temperature of 20°C were used to simulate a stratified impoundment. The flow was made visible using the shadowgraph technique. Typical photographs obtained during the middle and later stages of the mixing process are shown in Fig 5. Cold water, pumped from the base of the tank by the "bubble gun", mixed with the warm surface layers in the turbulent jet issuing from the exit of the stack pipe. Turbulent motion, induced by the jet and by the bursting air bubbles at the free surface, spread throughout the warm water layer. In the early and middle stages of the mixing process the pumped cold water moved down to the interface in the region close to the gun (Fig 5 and Fig 6a). The interface is displaced downwards by the pumping action of the gun, and by turbulent erosion. As the interface approached the base of the tank, and the temperature difference between the warm layer and the cold water discharged from the stack pipe became small, a weak circulation pattern with an outflow towards the tank walls was induced into the upper layer (Figs 5,6b). The effect of tank size and gun location on the induced circulation will be discussed later.

Experiments in a medium size tank 8.1

First series of experiments were made in a 3.7 m x 7.3 m x 1.8 m deep laboratory tank, to assess both the pumping and the mixing efficiency of the bubble gun with D = 0.144 m and stack pipe length L = 1.33 m. Warm surface layers were produced by slowly discharging hot water on the top of a calm cold water layer. Flow patterns produced at the top of the stack pipe were observed using dye traces, and were found to be similar to those described in section 8 (see Figs 5 and 6).

The pumping performance and the mixing efficiency of the model gun were determined for a range of water inlet port gap sizes, G, (see Fig 4), and bubble release frequencies, f. Results of these experiments are presented later in conjunction with similar results obtained in a larger tank.

Experiments in a large tank 8.2

In order to obtain results with larger values of stack pipe length to diameter ratio than could be achieved in the smaller tank, and to minimise scale effects, a second series of experiments was conducted using guns with stack pipe diameter D = 0.139 m and 0.291 m in a tank 15 m x 15 m and 10 m deep.

Test facility, model bubble gun, instrumentation 8.3

The experiments were conducted in a 15 m x 15 m x 10 m deep concrete lined tank, shown in Fig 7. Bubble guns were suspended from the bridge positioned across the centre of the tank. A 10 HP electric compressor supplied air through a 25 mm diameter reinforced hose to the base of the bubble production devices, via variable orifice meters to measure the air supply Q_a (see Fig 4).

Water from the top of the tank could be circulated through a water heating boiler by a small submersible pump. This was used to set up warm water surface layers.

Two geometrically similar bubble production devices were manufactured from transparent pipes, with the internal diameters of chamber A equal to 0.139 and 0.291 m respectively. The dimensions of the bubble guns used are shown in Table 4, and the dimensions of the bubble production devices in Table 5. It was possible to assemble bubble guns with a range of length to diameter ratios by using different numbers of standard 1.22 m long flanged stack pipe sections. The area of the water inlet port could be altered by changing the gap size G. Following the results of the preliminary experiments in the medium size tank (section 8.2) measurements were made

at three ratios of G/D = 0.25, 0.50 and 1.0. The initial volume of the air bubble could be altered by adjusting the length of pipe C (see Fig 4). The measurements of pumping performance were conducted with an initial bubble volume equal to that of a spherical bubble having a diameter equal to the stack pipe diameter D.

Water velocities were measured at the centre of the stack pipe exit using a miniature propeller current meter. Mean water velocities were obtained by planimetry from a chart recording of the current-meter output. The air supply Q_a was measured with standard variable orifice meters, and was in reasonable agreement with the value obtained from the measurements of the internal volume of the bubble production device and the bubble release frequency.

Water temperatures were measured using thermisters mounted on three vertical arrays. These were located on a diagonal line from the centre of the tank to one corner. The distance from the centre of the tank to each array was 2.4 m (Array 1), 5.1 m (Array 2) and 8.0 m (Array 3). Thermisters were mounted with a vertical spacing of 0.279 m on Arrays 1 and 2 and 0.328 m on Array 3. Thermister outputs were recorded with a data logging system scanning at ten channels per second. The punched paper tape output was processed to yield the mean and root mean square temperature for each thermister scanned.

PUMPING EFFICIENCY ANALYSIS 9

The pumping efficiency of the bubble guns was determined under isothermal conditions (no temperature stratification) and the parameters that affect the water discharge Q_W, measured at the exit of the stack pipe, can be listed as:—

Quantity	*Symbol*	*Units*
Mean water discharge at the stack pipe exit	$\bar{Q}_W$	$m^3\ s^{-1}$
Air supply at submergence h (see Fig 4)	Q_a	$m^3\ s^{-1}$
Submergence depth	h	m
Stack pipe diameter	D	m
Stack pipe length	L	m
Inlet water port gap†	G	m
Length of chamber C* (see Fig 4)	l	m
Bubble release frequency	f	s^{-1}
Bubble terminal velocity	U_B	$m\ s^{-1}$
Representative tank width	W	m
Mass density of water	ρ_w	$kg\ m^{-3}$
Mass density of air	ρ_a	$kg\ m^{-3}$
Acceleration due to gravity	g	$m\ s^{-2}$

† proportional to the area of the water inlet port
* proportional to the volume of the bubble on release

The equation indicating the relationship between the above parameters can be written as:—

$$f(\bar{Q}_W\ ,\ Q_a\ ,\ h,D,L,G,l\ ,f,U_B,W,\rho_w,\rho_a,g) = 0 \qquad ....(1)$$

Equation (1) can be written in the following form, making use of the theory of dimensions.

$$\frac{\bar{Q}_W}{Q_a} = \phi_1\left(\frac{U_B}{\sqrt{gD}}, \frac{f\,G}{\sqrt{gL}}, \frac{G}{D}, \frac{L}{D}, \frac{l}{D}, \frac{h-L}{D}, \frac{W}{D}, \frac{p_a + \rho_w gh}{p_a}, \frac{\rho_w}{\rho_a}\right) \quad \ldots(2)$$

In equation (2) the parameter $U_B/\sqrt{gD}$ represents the non-dimensional bubble rise velocity, U_B being the difference between total air bubble rise velocity and the ambient water velocity. The results of a subsidiary experiment showed that $U_B/\sqrt{gL}$ = a constant K. A mean value for K, K = 0.37, was determined from the experimental results. This is in reasonable agreement with K = 0.34 quoted for a large air bubble rising in a water-filled tube with zero ambient water velocity (Ref 44). The parameter $f\,G/\sqrt{gL}$ represents the non-dimensional bubble frequency and G/D and L/D the bubble gun geometry. For geometrically similar models of gun the parameter l/D represents the volume of the bubble production device. This parameter was constant and equal to 0.78 for the pumping efficiency measurements and its effect investigated in a second experiment described later. The parameters $\frac{h-L}{D}$ and W/D represent the location of the device below the free surface and the tank geometry respectively. For these experiments (h—L) was constant and equal to 1.0 m, and W was large enough for its effect on pumping performance to be negligible. The importance of both these parameters, with regard to efficiency of destratification, will be discussed later. The parameter

$$h^* = \frac{p_a + h\rho_w g}{p_a}$$

where p_a is atmospheric pressure, is the non-dimensional pressure ratio used to determine the air supply Q_A' at atmospheric pressure, eg

$$Q_A' = Q_a \times h^* \quad \ldots(3)$$

The mean water discharge $\bar{Q}_W$ was calculated from the relationship

$$\bar{Q}_W = \frac{\alpha \bar{U}_W \pi D^2}{4} \quad \ldots(4)$$

where α is a constant, assumed equal to unity, and $\bar{U}_W$ is the centre line mean water velocity, measured at the exit of the stack pipe. $\bar{U}_W$ was determined over a period equivalent to ten bubble releases.

Equation (2) can be written in the form:—

$$\frac{\bar{Q}_W}{Q_A'} = \phi_2\left(\frac{U_B}{f(\rho_w/\rho_a)\sqrt{gD}}, \frac{f\,G}{\sqrt{gL}}, \frac{G}{D}, \frac{L}{D}, \frac{l}{D}, \frac{h-L}{D}, \frac{W}{D}\right) \quad \ldots(5)$$

the $f(\rho_w/\rho_a)$ does not change very much for the range of temperatures encountered in these experiments and is assumed to be constant.

Water velocity U_W at the stack pipe exit 9.1

The variation in the water velocity, U_W, with time in a typical test is shown for two bubble release frequencies in Fig 8. This shows that the water in the stack pipe is accelerated at an almost constant rate during the air bubble rise. The water velocity decays when the bubble has left the stack pipe, until the next bubble is released and the cycle is repeated. The decay period can be reduced by decreasing the bubble release frequency f.

Pumping efficiency results 9.2

The non-dimensional parameters $\bar{Q}_W/Q_A'$, f $G/\sqrt{gL}$, L/D and G/D were determined experimentally and are shown in Fig 9, where $\bar{Q}_W/Q_A'$ is shown as a function of f $G/\sqrt{gL}$ for three different values of the gap ratio G/D. This figure also shows data for a 0.144 m diameter bubble gun obtained in the intermediate rise tank experiments (see Table 4).

The results shown in Fig 9 indicate that the non-dimensional parameters given in equation (5) can be used to represent the pumping performance of the device when the L/D ratio is larger than 9.2. At small values of L/D the pumping efficiency becomes more dependent on the finite time taken for the large bubble to form at the base of the stack pipe. It was observed that the large bubble does not form and fill the stack pipe until the air released from the bubble production device has risen several stack pipe diameters. However the results obtained at $L/D \leqslant 9.2$ are not of great practical interest for the destratification application, as the pumping efficiency is small at small values of L. This can be seen from Fig 9, but is shown more clearly in Fig 10 where the mean water velocity $\bar{U}_W$ is plotted against stack pipe length L for various bubble frequencies. Fig 10 shows that $\bar{U}_W$ increases with increasing L and will reach a maximum value asymptoticly at some value of $L > 7$ m.

Fig 9 further shows that increasing the area of the water inlet port from that represented by the parameter G/D = 0.5 to G/D = 1.0 has no significant effect on pumping efficiency. Thus the gap size G can be chosen to be large enough for its effect to be small. Fig 9 can be used as the basis of a design method for large bubble guns as described in Appendix A. A comparison of the pumping performance results with data presented by Bryan (Ref 21) for the "Aero-Hydraulics Gun" is shown in Appendix B.

The effect of bubble volume on pumping performance 9.3

It was shown (Ref 21) that the pumping performance of a large air bubble gun is strongly affected by the size of the air bubble. In view of this, the pumping performance experiments were conducted with the dimensions of the bubble production device (see Fig 4) scaled to produce bubbles of a similar volume, in relation to the stack pipe diameter, as were used in the Aero-Hydraulics Gun (Refs 21 and 45). However, preliminary experiments with a 25 mm diameter model bubble gun indicated that large variations in the initial bubble volume had only a small effect on the volume of water pumped per bubble.

The effect of variations in l/D on the volume of water pumped per bubble released is shown in Fig 12, where $\bar{Q}_W/f$ is plotted against f for three values of l/D. Fig 12 shows that large changes in l/D produce only small changes in $\bar{Q}_W/f$, the value of $\bar{Q}_W/f$ increasing slightly with increasing l/D. The practical significance of variations in l/D is best seen by relating the volume of water pumped to the volume of air supplied. In Fig 12, water discharge $\bar{Q}_W$ has been plotted against Q_A' for three values of l/D. This figure shows that variations of l/D have only a small effect on the pumped discharge when this is related to the volume of air supplied.

Destratification experiments 9.4

A series of experiments were conducted to study the mixing efficiency of air bubble guns with two different diameters in thermally stratified layers. Warm surface layers were set up artificially in order to simulate the density stratification that occurs in lakes and reservoirs. The temperature difference between cold and warm water used in the experiments was similar to that usually occurring in prototype. The water heating boiler and circulating pump used being operated continuously for six hours to produce a warm layer one metre deep with a temperature difference of 10^{o}C. The exit of stack pipe was positioned one metre

below the free surface, ie in the thermocline. In lakes and reservoirs the depth of epilimnion is usually larger than one metre (see section 2.1). Hence the non-dimensional parameter $\frac{h-L}{D}$ is much higher than 3.4 and 7.2 used in the experiments presented here. The effect of $\frac{h-L}{D}$ and of tank size on the results will be discussed later.

The experimental tank was initially mixed to obtain isothermal conditions. Water in the top layer was then recirculated via the water heating boiler until the required warm surface layer was produced. The experiment was started after one hour, in order to allow disturbances in the warm layer to decay. Vertical temperature profiles were recorded from the water surface to a point below the thermocline. Data was obtained for two minute periods, at ten to twenty minute intervals, depending on the rate at which the thermocline moved. From the experimental data mean temperatures and root mean square (rms) temperature fluctuations were evaluated for each test.

The rms values, T', were made dimensionless by using $\overline{T} = \frac{1}{N} \sum_{n=1}^{N} t_n$ as temperature scale, where N is number of digitized values of temperature t_n taking at each point.

Fig 13 shows mean temperature profiles, turbulent intensity profiles of temperature fluctuation, measured in a typical test. Similar results were obtained in all the tests and showed that, below the thermocline, the mean temperature remained constant and that rms values were small. The thermocline, (see section 2.1), is characterised (a) by a large mean temperature gradient in the vertical direction and (b) by a maxima in the rms temperature profiles. Above the thermocline and near the free surface mixing of the cold water pumped by the device results in small mean temperature gradients and rms temperature fluctuations. Small lateral temperature gradients, typically 0.2°C to 0.4°C, were also observed between thermister Arrays 1 and 2, (see section 8.3.1), during the early stages of the mixing process.

Rate of thermocline movement 9.5

This was determined using the maxima in the turbulent intensity profiles to estimate the position of the density interface (thermocline) at known times. Fig 14 shows the position of the interface plotted against time for three different values of bubble release frequency, f. Fig 14 shows that the interface was depressed at a constant rate, which increased with increasing bubble release frequency, and that the thermocline remained in a horizontal plane during the mixing process.

Thermocline movement due to turbulent erosion 9.6

The downwards movement of the thermocline during the mixing process can be attributed to the two following effects:–

a) The thermocline is depressed as water is transferred in the stack pipe from the base of the tank (hypolimnion), and mixed with the warm surface layers (epilimnion).

b) The thermocline is eroded from above by the turbulent motion induced in the warm water layer. (Turbulence in the upper layer can also be developed by wind action. An experiment conducted during a period of high winds, without artificial mixing. It was found that wind generated turbulent erosion in the long tank was negligible.)

The magnitude of turbulent erosion can be quantified by an entrainment velocity, U_e. If U_p is defined as the rate of interface movement due to pumping action only, U_e is the difference between the measured rate of interface movement, U_i, and, U_p. Appendix C shows the calculation used to determine U_e from the measured data.

Table 6 shows the test conditions and entrainment velocities determined in five experiments conducted in the 15 m x 15 m x 10 m test tank, together with some of the data determined in the medium size tank experiments described in section 8.1.

The volume of hypolimnion water effectively transferred across the thermocline by turbulent erosion, Q_e, can be calculated from:–

$$Q_e = U_e \times A \qquad \ldots.(6)$$

In order to determine the relationship between Q_e and the pumped discharge $\bar{Q}_W$ the measured values are plotted in Fig 15 for the runs listed in Table 6. The following relation can be written as a best fit to the experimental data.

$$Q_e = k \times \bar{Q}_W^{\,n} \qquad \ldots.(7)$$

where k and n are dimensional constants in the SI system of units. It appears from the rather sparse data shown in Fig 15 that n = 2.4 was the same in the medium and large tank experiments. The constant k was different for experiments in different tanks, $k \approx 700$ and $k \approx 31$ in the medium and large tanks respectively. The constant k will depend on tank geometry and gun location, and on the temperature difference between the hot and cold layers (see the test 6 result).

Appendix D shows a correlation of the measured entrainment velocities U_e with a parameter having the same form as a Richardson number.

Turbulent erosion causes the thermocline to propagate downwards at a faster rate than would occur from the pumping action of the air bubble gun. The "effective" pumping efficiency, when a bubble gun is used to mix temperature stratified layers, can be defined as Q_i/Q_A' where $Q_i = U_i \times A$, and Q_A' is as defined in section 9. The ratio Q_i/Q_A' is plotted in Fig 16 against the parameter $f \times G/\sqrt{gL}$ (dashed line). Also shown in this figure is the ratio $\bar{Q}_W/Q_A'$, determined from the water discharge at the stack pipe exit (solid line). This figure shows the effect of turbulence generated in the warm water layer on the pumping performance of the bubble gun. When the pumped discharge is small, ie the 0.291 m diameter gun operating at a low bubble release frequency, f, or the 0.139 m diameter gun operating at a high f, turbulent erosion is also small, due to weak turbulent motion. In this case Q_i/Q_A' approaches $\bar{Q}_W/Q_A'$. An increased bubble release frequency, resulting in an increased pumped discharge, and in turn to increased turbulent erosion, results in Q_i/Q_A' becoming progressively larger than $\bar{Q}_W/Q_A'$. Furthermore, the results obtained in tests 3 and 6 (see Table 6 and Fig 16), indicate that an increased initial temperature difference leads to increased damping of the turbulent motion, and to a decrease in turbulent erosion.

Experiment with a small air bubble mixing device 9.7

A preliminary experiment was conducted in the 15 m x 15 m x 10 m deep tank to evaluate the mixing efficiency of a device producing small air bubbles. This test was conducted with an air supply rate of 0.008 $m^3 s^{-1}$, with an initial warm layer depth of 1.0 m, and an initial temperature difference of 10^oC. These conditions were similar to those for test 4 in the bubble gun experiments (Table 6).

Small air bubbles were released as a plume from a 25 mm diameter diffuser pipe 2 m long, containing 27 small holes, 1 mm diameter, at a spacing of 75 mm. The hole size and spacing were the same as one of the diffusers used by Kobus (Ref 32).

The movement of the interface was determined as described previously, (section 9.5), and found to be larger than that measured in the large bubble gun test 4. Table 7 shows the results obtained in the two experiments, the parameter Q_i/Q_A' (see section 9.7) being used to compare the

effective efficiency of destratification of the two systems. Although the Q_i/Q_A' obtained with the small bubble device appears much larger than that measured in the equivalent large bubble gun experiment the comparison is complicated by the following factors:–

A A flow visualisation experiment, conducted in the tank described in section 8.1, showed that a modelled diffused air device produced a strong circulation in the warm layers, as sketched in Fig 17. The strength of the induced circulation pattern was obviously affected by the presence of the tank walls. Rouse, (Ref 46), has investigated the flow patterns produced by a vertical jet in a rectangular tank and found that the circulation pattern depends strongly on the ratio W/H when $W/H < 2.5$. (W is the tank half width); W/H was about 0.8 for the results given here, and this resulted in a strong return flow at the interface and increased turbulent erosion. In a prototype installation W/H will be large, and thus the tank results can be expected to overestimate the mixing efficiency of the small bubble device.

B In the bubble gun experiments the non-dimensional parameter of submergence $\frac{h-L}{D}$ was ≈ 3 or 7, and energy losses occur as the turbulent jet issuing from the stack pipe impinges the free surface, causing a large surface boil. In a prototype installation $\frac{h-L}{D}$ will often be larger than was the case for the tank experiments, and a large proportion of the momentum of the turbulent jet will be dissipated in mixing processes in the warm layer

The comparison between the small and large air bubble mixing devices was thus distorted by the test conditions and should be accepted with reserve.

CONCLUSIONS 10

1 Artificial destratification has been used successfully as a method of water quality control in stratified impoundments. A variety of mixing methods, including raft mounted pumps, pumped water jets, and air bubble mixing devices have been used.

2 The parameters used to compare the efficiency of mixing devices have limitations, and these make a clear-cut comparison of different mixing methods difficult. However, air bubble mixing appears to have produced the largest operating efficiencies, and may offer practical advantages for installations in existing impoundments.

3 Hypolimnion Aeration devices have been developed for water quality improvement in stratified impoundments where artificial destratification may be unacceptable. One study suggests that small-bubble full-airlift devices offer the lowest capital and operating costs.

4 The use of artificial destratification as a technique for reducing evaporation in deep stratified impoundments has been suggested. More work is required to validate the claims made for this method of evaporation control.

Conclusions from present experiment

5 The pumping performance of large air bubble guns has been investigated in laboratory and near prototype scale experiments. The results obtained form the basis of a design method for large bubble guns.

6 The discharge from a large air bubble gun increases with increasing stack pipe diameter, and air bubble release frequency. Discharge increases with increasing stack pipe length and will reach a maximum value asymptoticly at some value of $L/D > 52$. The pumping efficiency, defined as the ratio

of the volume of water pumped to the volume of air supplied, decreases with increasing air supply. The water discharge per air bubble released is not strongly affected by the volume of the bubble production device, provided the bubble fills the stack pipe.

7 Turbulent erosion increases the rate of mixing of temperature stratified layers mixed with a bubble gun. In tank experiments, when the pumped discharge is large in comparison with the tank volume, turbulent erosion can be responsible for a significant part of the rate of thermocline movement. The measured entrainment velocities have been correlated with a parameter having the same form as Richardson Number.

8 A comparison between a large bubble gun and a small bubble mixing device showed that, in a tank, small bubble mixing was more efficient. The test conditions did not, however, represent a reservoir condition and more work would be required before a valid comparison could be made.

ACKNOWLEDGEMENTS 11 This work was carried out by Mr P Lawrence in Dr H O Anwar's section of the Hydraulic Research Station's Overseas Unit, which is headed by Mr D R P Farleigh. The co-operation of the staff of Ames Crosta Ltd, whose test tank facility was used for some of the experiments, is gratefully acknowledged. Miss A L Taylor assisted in the preliminary experimental programme and in the design of the large bubble guns; Mr J Coles assisted in the large test tank experimental programme and Mr R Atkins was responsible for the data reduction programmes.

REFERENCES 12

1 Collingwood R W, Water storage and reservoir management, their effect on water quality. Association of River Authorities Year Book, 1966, pp 24-34.

2 Tekeshi Ito, Mixing method of stratified water layer in reservoirs. International Symposium on Stratified Flows, Novosibirsk, 1972, pp 567-577.

3 Lack T J and Coolingwood R W, The control of reservoir water quality by engineering methods. Proceedings of WRC Symposium on The Effects of Storage on Water Quality, March 1975, Paper 18.

4 Churchill M A, Effects of storage impoundments on water quality. Proc ASCE, SA1, February 1957.

5 Symons J M, Carswell J K and Robeck C G, Mixing of water supply reservoirs for quality control. J American Water Works Assoc, **62**, pp 322-334.

6 Irwin W H, Symons J M and Robeck G G, Impoundment destratification by mechanical pumping. Proc ASCE, **92**, SA6, December 1966.

7 Quintero J E and Garton J E, A low energy lake destratifier. Trans Am Soc Agric Engrs, **16**, October 1973, pp 973-976;

8 Bernhardt H, Aeration of Wahnbach Reservoir without changing the temperature profile. Jnl Amer Water Wks Assoc, **59**, Part 9, 1967, pp 943-949.

9 Symons J M, Irwin W H, Robinson E L and Robeck G G, Impoundment destratification for raw water quality control using either mechanical or diffused air pumping. Jour AWWA, **59**: 1268 (1967).

10 Knoppert P L, Rook J J, Hofker J J and Oskam G, Destratification experiments at Rotterdam. 5 Am Water Wks Assoc, **62**, 1970, pp 448-454.

11 Tolland H G, Rearation and destratification of Hawkridge Reservoir. WRC ER 446, September 1976.

12 Rapoza D, Reservoir aeration improves water quality. Public Works, **102**, Part 5, 1971, pp 86-87.

13 Ogborn C M, Aeration system keeps water testing fresh. Public Works **97**, April 1966, pp 84-86.

14 Verner B, Pneumatic oil barriers. Atlas Copco, Tryckluft 1, 1972.

15 Bengtsson L and Geliw C, Artificial aeration and suction dredging methods for controlling water quality. Proceedings of WRC Symposium on The Effects of Storage on Water Quality, March 1975, Paper.

16 Heath W A, Compressed air revives polluted Swedish lakes. Water and Sewage Works, May 1961, pp 200.

17 Moretti P M and McLaughlin D K, Hydraulic modelling of mixing in stratified lakes. Proc ASCE, **103**, HY4, April 1977.

18 Lackey R T, A technique for eliminating thermal stratification in lakes. Paper No 72005, Water Resources Bulletin, 8, No 1, February 1972, pp 46-49.

19 Wirth T L, Mixing and aeration systems in Wisconsin Lakes. Symposium on the Management of Midwestern Winterkill Lakes, Winnipeg, Manitoba, Canada, December 1970.

20 Polycon Environmental Control Systems Ltd. Helixor promotional literature.

21 Bryan J G, Physical control of water quality. J Brit Watwks Assn August 1964, pp 546-564.

22 Symons J M (Chairman), A committee report. Quality control in reservoirs for municiple water supplies. Quality Control in Reservoirs Committee, American Water Works Association, May 1971.

23 Neilson B J, Re-aeration dynamics of reservoir destratification. J American Water Works Association, 1974 pp 617-620.

24 Symons J M, Impoundment water quality changes caused by mixing. Proc ASCE, SA1, April 1967.

25 Steel J A, The management of Thames Valley reservoirs. Proceedings of WRC Symposium on The effects of Storage on Water Quality, March 1975, Paper 14.

26 Ridley J E, Cooley P and Steel J A, Control of thermal stratification in Thames Valley reservoirs. Proc Soc Wat Treat Exam, 1966 **15**, pp 225-244.

27 Symons J M, Management and measurement of D.O. in impoundments. Proc ASCE, SA6, December 1967.

28 Koberg G E and Ford M E, Elimination of thermal stratification in reservoirs and the resulting benefits. Geol Surv Wat Supp, Paper 1809-M US Govt Printing Office, 1965.

29 Thrackston E L, Discussion "Impoundment destratification by mechanical pumping". ASCE, **93**, SA2, April 1967.

30 Gebhart G E and Summerfelt R C, Effects of destratification on the depth distribution of fish. Proc ASCE EE6, December 1976.

31 Steichen J M, The effect of lake destratification on water quality parameters. Thesis presented to the Oklahoma State University, at Stillwater, Okla, 1975. [Cited in Ref].

32 Kobus E K, Analysis of the flow induced by air bubble systems. Proc XIth International Conference on Coastal Engineering, London, September 1968.

33 Cederwall K and Ditmars J D, Analysis of air bubble plumes. Wm Keck Laboratory of Hydraulics and Water Resources, Division of Engineering and Applied Science, California Institute of Technology, Pasadena, California. Report No KH–R–24, September 1970.

34 Wirth T L and Dunst R C, Limnological changes resulting from artificial destratification and aeration of an impoundment. 28th Midwest Fish and Windlife Conference, Chicago, USA, Dec–11–14, 1966.

35 Wirth T L, Mixing and aeration systems in Wisonsin Lakes. A Symposium on the Management of Midwestern Winterkill Lakes, Winnipeg, Manitoba, Canada, December 1970.

36 Fast A W, Dorr V A and Rosen R J, A submerged hypolimnion aerator. Water Resources Research, **11**, No 2, April 1975.

37 Fast A W, Lorenzen M W and Glen J H, Comparative study with costs of hypolimnetic aeration. Proc ASCE, EE6, December 1976.

38 Fast A W and Lorenzen M W, Synoptic survey of hypolimnetic aeration. Proc ASCE, EE6, December 1976.

39 Speece R E, The use of pure oxygen in river and impoundment aeration. Presented at the 1969 24th Indiana Waste Conference, held at Purdue University, Lafayette, Ind, USA.

40 Fast A W, Overholtz W J and Tubb R A, Hypolimnetic oxygenation using liquid oxygen. Water Resources Research, **11**, No 2, April 1975.

41 Bernhardt H, Ten years experience of reservoir aeration. Presented at the 7th International Conference on Water Pollution Research, Paris, France, 9-13 September 1974.

42 Fast A W, Effects of artificial destratification on primary production and zoobenthos of El Capitan Reservoir, California. Water Resources Research, **9**, No 3, June 1973.

43 Hughes T C, Richardson E A and Franckiewicz J A, Evaporation suppression by reservoir destratification. Water salvage potentials in Utah, **11**, PRWA22–2, Utah Water Research Laboratory, Utah State University, Logan, Utah 84322, USA, June 1975.

44 Batchelor G K, An introduction to fluid dynamics. Cambridge University Press, 1967.

45 Aero-Hydraulics Limited, AHG promotional literature.

46 Iamandi C and Rouse H, Jet induced circulation and diffusion. Proc ASCE, **96**, HY1, January 1970.

47 Hinze J O, Turbulence. 2nd edition, McGraw-Hill Inc, 1975.

48 Thorpe S A, Turbulence in stably stratified fluids. A review of laboratory experiments boundary layer. Meteor 5 95.

49 Crapper P F and Linden P F, The structure of turbulent density interfaces. J Fluid Mech, **65**, part 1, August 1974.

50 Brezonik P L, Delfino J J and Lee G F, Chemistry of M and MN in Cox Hollow Lake Vis., Following Destratification. Proc ASCE SA5 October 1969.

APPENDICES

APPENDIX A

Design method for aero-hydraulic guns

The design method is based on the pumping performance of aero-hydraulic guns (AHG), the effects of turbulent erosion being ignored. The effects of turbulent erosion in an impoundment, particularly due to wind action, will often be difficult to predict without preliminary field measurements. In some cases a design based on pumping performance will be conservative, as turbulent erosion of the thermocline will result in destratification being achieved more rapidly than would be expected from a consideration of the pumped water volumes.

Choice of AHG dimensions and bubble release frequency

Aero-hydraulic guns are placed with the top of the stack pipe at the thermocline before mixing commences. This will usually determine the length of stack pipe (L) to be used. The effects of the variation in the other physical dimensions of the bubble guns are described in sections 9.3 and 9.4. Use of a low bubble release frequency, f, will increase the pumping efficiency, but as the water discharge per bubble gun is then low, a larger number of AHG's will be required to achieve a given volumetric pumping rate.

Determination of the pumped water discharge and the number of AHG required

The total water discharge required can be calculated from:—

$$\bar{Q}_W \text{ (TOTAL)} = \frac{V}{t} \qquad \text{....(A1)}$$

where V is the hypolimnion volume and t is the required mixing time. A mixing technique involving a rapid initial destratification followed by intermittent use of the mixing device to maintain an impoundment in a fully mixed state has been recommended (Ref 9). Mixing times are typically in the range several days to several weeks.

Q_A' per AHG device is calculated from

$$Q_A' = f \times V_s \times \frac{L + 1.0 + 10.4}{10.4} \qquad \text{....(A2)}$$

where V_s is volume of the siphon (see Fig 4) and 10.4 in the atmospheric pressure.

Note that equation (A2) assumes that the exit of the stack pipe is positioned 1 m below the free surface. The effect of an increase in this depth is discussed in the next section.

For a given Q_A' the water discharge $\bar{Q}_W$ can be calculated from the ordinate of Fig 9, using the parameter, $f \times G/\sqrt{gL}$, calculated from the chosen physical dimensions of the bubble gun. The number of AHG required is then given by:—

$$N = \frac{\bar{Q}_W \text{ (TOTAL)}}{\bar{Q}_W} \qquad \text{....(A3)}$$

At this stage it may be necessary to revise the choice of the physical dimensions of the gun, the bubble release frequency or the mixing time, t, to produce an acceptable design. The "optimum" design for a particular installation will depend on economic as well as technical factors and can only be determined with the knowledge of specific local circumstances.

Having determined the final number and arrangement of bubble guns the air compressor duty can be specified from:—

$$Q_A = N \times V_s \times f \qquad \text{....(A4)}$$

The volume Q_A must be supplied at a pressure P given by:–

$$P = \rho_w g[10.4 + L] \quad \text{....(A5)}$$

An allowance should also be made for the pressure loss in air supply pipes and fittings, but this will usually be small in comparison with the hydrostatic head at the bubble production device.

Effect of large $\frac{h-L}{D}$

The design procedure outlined previously assumes that the distance from the top of the stack pipe to the free surface is h–L = 1 m. In a prototype installation h–L will often be larger than 1 m, and $\frac{h-L}{D}$ will be large in comparison with the values applying for the pumping performance measurements on which Fig 9 is based. An increase in $\frac{h-L}{D}$ will have a number of effects:–

a) Entrainment by the turbulent jet produced at the stack pipe exit will increase the total volume of water brought to the surface zone, although the volume of water transferred across the thermocline remains the same. The volume flux at a height, Z, above the axis can be estimated from:–

$$\frac{\bar{Q}_{W(Z)}}{Q_W} = \alpha[\frac{Z + a}{D}] \quad \text{....(A6)}$$

Hinze (Ref 47) gives values of $\alpha = 0.32$ and $a = 3D < a < 7D$.

Entrainment of epilimnion fluid will decrease the density difference between the jet and the ambient fluid and will reduce the tendency of the pumped hypolimnion water to sink back to the thermocline.

b) An increase in submergence depth, with all the other factors the same, will result in a decrease in the ratio of the bubble volume at the stack pipe exit to the bubble volume at the point of release. Table 8 shows bubble volume ratios calculated for two values of $\frac{h-L}{D}$ and three values of L. As the gas law describing the bubble expansion is not known, values are tabulated for isothermal and adaibatic bubble expansions. Table 8 shows that changes in bubble volume ratio due to an increase in h–L are not large. These changes will not significantly affect the discharge (see section 9.4), and the design procedure outlined previously which assumes that h–L = 1 m can be used. However, the air compressor must be specified using the submergence depth h from which the bubbles are to be released.

APPENDIX B

Comparison of the pumping performance results with the aero-hydraulics gun

The only other data available on the performance of large aero-hydraulics guns (AHG) is that presented by Bryan (Ref 21) where the performance graphs for AHG with diameters of 0.3 m and 0.45 m are shown. Bryan's data for the 0.3 m diameter gun can be replotted in non-dimensional form by deriving a bubble release frequency from the quoted air supply rates and by assuming that the initial bubble volume was that quoted in Ref 45. An equivalent gap size was determined from the drawing shown in Ref 24.

A comparison between Bryan's results and those obtained in this investigation is shown in Fig 18. In this figure the dashed lines showing a best-fit to the data obtained from measurements presented in this report. Fig 18 shows at small values of L/D, reasonable agreement between the Bryan AHG data obtained at an equivalent gap ratio of G/D of 0.47, and the HRS G/D = 0.5 result. However, the Bryan AHG data shows a progressive decrease in pumping efficiency as L/D increased, and this trend was not observed in the present measurements (see Fig 10).

APPENDIX C

Calculation of entrainment velocity

For a rectangular tank, and a small density differences used in experiments presented in this report the following relation can be written.

$$\bar{\rho}\ A\ U_e + \bar{\rho}\ \bar{Q}_W = -\ A\ \bar{\rho}\ \frac{dy}{dt} \qquad \text{....(C1)}$$

where

$\bar{\rho}$ = mean water density kg m^{-3}

A = tank cross-sectional area m^2

U_e = mean entrainment velocity m s^{-1}

y = height of the interface from the floor m

t = time s

hence

$$U_e = -\frac{dy}{dt} - \frac{\bar{Q}_W}{A} \qquad \text{....(C2)}$$

dy/dt and $\bar{Q}_W$ are measured quantities and A is known. Note that check measurements showed that the pumped discharge Q_W was not significantly affected by the presence of the density stratification.

APPENDIX D

Correlation of measured entrainment velocities

Turbulent erosion at a density interface has been investigated by a number of workers, usually in laboratory scale experiments and for situations with and without a mean shear force parallel to the interface (eg Ref 48). Entrainment velocities have been correlated with different forms of Richardson number, although the Peclet number is also important when molecular diffusion effects are significant (Ref 49).

It was hoped that the results from large tank could be correlated in the form:–

$$\frac{U_e}{U_r} = K\left[\frac{g\Delta\rho L}{\rho U_r^2}\right]^n \qquad \text{....(D1)}$$

where U_r and L are a velocity scale and a length scale respectively. Unfortunately the results from an electro-magnetic current used to obtain U_r and L proved to be unreliable. However it is possible to correlate the entrainment velocities measured in the tank experiments with a parameter having the same form as Richardson number by making some assumptions.

a) The length scale is some constant fraction of the warm layer depth, and can be represented by the epilimnion thickness.

b) The scale velocity can be defined as:–

$$U_r = U_p = \frac{\bar{Q}_W}{A}$$

As U_p is constant for each run, and from conservation of mass the product $\Delta\rho H$ is also constant, each experiment represents one value of the parameter R_i'

$$R_i' = \frac{g\ \Delta\rho_o\ H_o}{\rho\ U_p^2} \qquad \text{....(D2)}$$

In equation (D2) $\Delta\rho_o$ and H_o are the initial warm layer density difference and depth respectively. It should be noted that although R_i' has the same form as the physically correct Richardson number it is numerically larger. This is a consequence of the definition adopted for U_p. [A similar parameter was used by Maretti, Ref 17, to correlate the results of modelled and prototype destratification experiments.]

The ratio U_e/U_p determined in the medium and large tank experiments is plotted against R_i' in Fig 20, together with three points obtained in the tank described in section 8.1. A best fit through this data yields:

$$\frac{U_e}{U_p} = 1.46 \times 10^4\ R_i'^{-0.82} \qquad \text{....(D3)}$$

Equation (D3) correlates entrainment velocities measured in tanks having a width between 0.76 m and 15 m.

TABLES

TABLE 1 COMPARISON OF DESTRATIFICATION SYSTEMS

Impoundment	Volume (m^3)	Max depth (m)	System	DE %	OC (Kg 0_2/KWH)	Energy input Unit volume (KWH/m^3)	Notes
Boltz Lake (USA)	3.6×10^6	18.9	Mech pump	0.2 (a)	0.6	4.0×10^{-3}	Raft mounted pump
Vesuvius Lake (USA)	1.6×10^6	9.1	Mech pump	0.4 (a)	–	1.2×10^{-3}	Raft mounted pump
King George IV Reservoir (UK)	20.2×10^6	16.0	Mech pump	0.1 (b)	–	1.6×10^{-3}	Raft mounted pump
Cox Hollow Lake (USA)	1.47×10^6	8.5	Aero-hydraulics gun	0.4 (b)	0.6	1.5×10^{-3}	OC quoted by Bryan (Ref 21) not measured in Cox Hollow Lake
Boltz Lake (USA)	3.6×10^6	18.9	Diffused air	0.6 to 1.5 (a)	1.0 to 4.3	5.9×10^{-4}*	*Average from 4 mixings
Falmouth Lake (USA)	5.67×10^6	12.8	Diffused air	0.2 to 0.9 (a)	0.0 to 4.2	5.6×10^{-4}*	*Average from 5 mixings
Wahnbach Reservoir (West Germany)	41.6×10^6	43.0	Diffused air	0.4 (b)	0.5	2.5×10^{-3}	OC from oxygen transferred from bubbles to water, does not include surface creation
Lake Wohlford (USA)	3.1×10^6	15.2	Diffused air	0.5 (b)	–	8.2×10^{-4}	
Maarsseveen (Holland)	8.0×10^6	30.0	Diffused air	1.1 (b)	–	–	Diffused air from perforated tube at depth 19 m
Maarsseveen (Holland)	8.0×10^6	30.0	Diffused air	1.1 (b)	–	–	Single diffuser (162 x 1.2 mm dia holes) at depth 30 m
Vaxjosjon (Sweden)	3.1×10^6	6.5	Diffused air	–	0.5	1.9×10^{-4} (estimated)	Diffused air from perforated pipe

Notes:– (a) Corrected for natural stability changes. (b) Not corrected for natural stability changes, DE = destratification efficiency.

TABLE 2 COMPARISON OF HYPOLIMNION AERATION SYSTEMS

Impoundment	*Volume* (m^3)	*Max depth* (*m*)	*System*	*Oxygenation efficiency* (kgO_2/KWH)	*Notes*
Lake Waccabuc (USA)	4.1 x 10	13	Limno	0.54	Measured oxygenation efficiency. (Efficiency will depend on water depth)
—	—	—	Limno	0.95	Estimate only
Wahnbach Reservoir (West Germany)	41.6 x 10	43	Airlift	1.09	Measured oxygenation efficiency (Efficiency will depend on water depth)
Jarlasjon (Sweden)	7.8 x 10	24	Airlift	0.40	Measured oxygenation efficiency (Efficiency will depend on water depth)
Ottoville Quarry (USA)	0.06 x 10	18	SSP (Oxygen injection)	0.23	Measured oxygenation capacity
San Vicente Reservoir (USA)	1.11 x 10	58	SSP (Oxygen injection)	0.68	Estimate only

TABLE 3 EVAPORATION SUPPRESSION AS A FUNCTION OF IMPOUNDMENT MAXIMUM DEPTH AND FLOW INDEX

Tabulated values are % evaporation suppression for summer six months.
Source – Fig 16, Ref 43.

Impoundment maximum depth (m)	*Flow index = 0*	*0.3*	*0.7*
15.2	2.0	7.0	13.0
30.5	9.0	14.0	21.0
91.4	22.0	27.0	33.0

Note:–

1) Flow index = ratio of outflow to storage.

2) Slightly smaller values of suppression will be obtained on an annual basis.

3) Regression obtained using data from 10 impoundments.

TABLE 4 MODEL GUNS AND TANK DIMENSIONS

Flow visualisation experiments

Tank size 0.76 m x 0.76 m x 0.45 m deep

Gun size

Diameter (D) (m)	*Length (L) (m)*	*Gap (G) (m)*	*G/D*	*L/D*
0.025	0.23	0.007	0.28	9.0

Preliminary pumping performance experiments

Tank size 7.3 m x 3.7 m x 1.8 m deep

Gun sizes

Diameter (D) (m)	*Length (L) (m)*	*Gap (G) (m)*	*G/D*	*L/D*
0.144	1.33	0.013	0.09	9.2
0.144	1.33	0.025	0.17	9.2
0.144	1.33	0.051	0.35	9.2
0.144	1.33	0.102	0.71	9.2

TABLE 4 (Continued)

Large tank tests

Tank size = 15 m x 15 m x 10 m deep

Gun sizes

Gun	*Diameter (D) (m)*	*Length (L) (m)*	*Gap (G) (m)*	*G/D*	*L/D*
A	0.139	7.31	0.139	1.0	52.6
B	0.139	4.88	0.139	1.0	35.1
C	0.139	2.43	0.139	1.0	17.5
D	0.139	7.31	0.070	0.5	52.6
E	0.139	4.88	0.070	0.5	35.1
F	0.139	2.43	0.070	0.5	17.5
G	0.139	7.31	0.035	0.25	52.6
H	0.139	4.88	0.035	0.25	35.1
I	0.139	2.43	0.035	0.25	17.5
J	0.291	7.31	0.291	1.0	25.1
K	0.291	4.88	0.291	1.0	16.8
L	0.291	2.43	0.291	1.0	8.4
M	0.291	7.31	0.146	0.5	25.1
N	0.291	4.88	0.146	0.5	16.8
O	0.291	2.43	0.146	0.5	8.4
P	0.291	7.31	0.073	0.25	25.1
Q	0.291	4.88	0.073	0.25	16.8
R	0.291	2.43	0.073	0.25	8.4

TABLE 5 DIMENSIONS OF THE BUBBLE PRODUCTION DEVICES

The bubble production devices for D = 0.139 m and 0.281 m bubble guns were constructed from stock sizes of transparent tube. The principal dimensions of the devices were geometrically similar. Small differences in the internal volumes, due to the fixed wall thickness of stock tubing, were accounted for by a small adjustment in the length of the pipe C (see Fig 4), to produce internal volumes equal to $\frac{4[D/2]^3}{3\pi}$

Referring to Fig 4 the principal dimensions are:–

	Chamber A	*Chamber B*	*Pipe C*
$\frac{\text{Internal diameter}}{D}$	1.0	0.46	0.26
$\frac{\text{External diameter}}{D}$	1.05	0.52	0.3
$\frac{\text{Length}}{D}$	1.6	1.4	Variable
$\frac{X_1}{D}$	–	0.06	–
$\frac{X_2}{D}$	–	Variable	–

The lengths of chambers A and B were longer than necessary for the bubble volume used, in order to accommodate variations in bubble volume. For a prototype gun $X_2/D = X_1/D$ is recommended.

TABLE 6 ENTRAINMENT VELOCITIES

Results from 15 m x 15 m x 10 m deep tank

Test number	*Diameter (D) (m)*	$\frac{L}{D}$	$\frac{G}{D}$	*Bubble release frequency*	*(1)* h_o *(m)*	*(2)* ΔT^oC	*(3)* $U_i\ m\ s^{-1}$	*(4)* $U_p\ m\ s^{-1}$	*(5)* $U_e\ m\ s^{-1}$
4	0.291	25.1	1.0	0.034	0.90	12.0	0.000278	0.000213	0.00065
3	0.291	25.1	1.0	0.106	1.10	11.0	0.000764	0.000388	0.00037
5	0.291	25.1	1.0	0.148	1.00	11.0	0.000953	0.000432	0.00052
6	0.291	25.1	1.0	0.109	1.10	16.0	0.000647	0.000394	0.00025
8	0.139	52.6	1.0	0.184	1.00	10.0	0.000087	0.000079	0.000008

Results from 7.3 m x 3.7 m x 1.8 m deep tank

Test number	*Diameter (D) (m)*	$\frac{L}{D}$	$\frac{G}{D}$	*Bubble release frequency*	*(1)* h_o *(m)*	*(2)* ΔT^oC	*(3)* $U_i\ m\ s^{-1}$	*(4)* $U_p\ m\ s^{-1}$	*(5)* $U_e\ m\ s^{-1}$
A14	0.144	9.2	0.35	0.188	0.54	13.5	0.000307	0.000224	0.000083
A15	0.144	9.2	0.35	0.135	0.61	13.4	0.000266	0.000175	0.000091
A16	0.144	9.2	0.35	0.075	0.62	12.6	0.000148	0.000120	0.00003

Notes:– (1) Initial depth of the warm layer.
(2) Temperature difference between hot and cold layers (initial).
(3) Rate of interface movement.
(4) Rate of interface movement due to pumping action.
(5) Entrainment velocity.

TABLE 7 COMPARISON OF LARGE AND SMALL BUBBLE MIXING DEVICES

Mixing device	Q_A' $m^3\ s^{-1}$	h_o *(m)* *(1)*	ΔT ^oC	$\frac{Q_i}{Q_A'}$
0.291 m diameter bubble gun	0.00081	0.90	12.0	77.0
Small bubble diffuser	0.00089	1.0	10.0	469.0

(1) Initial depth of the warm layer.

Note: This comparison is distorted by the test conditions used and should not be taken as representing the relative pumping efficiencies of small and large air bubble devices in a prototype installation.

TABLE 8 BUBBLE VOLUME RATIOS

The calculated ratios of the volume of the bubble at the top of the stack pipe and on release from the bubble production device are tabulated below for three stack pipe lengths and two values of h−L/D. Ratios are shown assuming both isothermal and adiabatic bubble expansions.

	Isothermal expansion		*Adiabatic expansion*	
Stack pipe length (m)	$\frac{V_2}{V_1}\left(\frac{h-L}{D}=\frac{1}{D}\right)$	$\frac{V_2}{V_1}\left(\frac{h-L}{D}=\frac{5}{D}\right)$	$\frac{V_2}{V_1}\left(\frac{h-L}{D}=\frac{1}{D}\right)$	$\frac{V_2}{V_1}\left(\frac{h-L}{D}=\frac{5}{D}\right)$
5.0	1.44	1.33	1.30	1.22
15.0	2.32	1.97	1.82	1.63
25.0	3.19	2.62	2.29	1.99

Note: V_2 = Bubble volume at top of stack pipe.

V_1 = Bubble volume on release from the bubble production device.

FIGURES

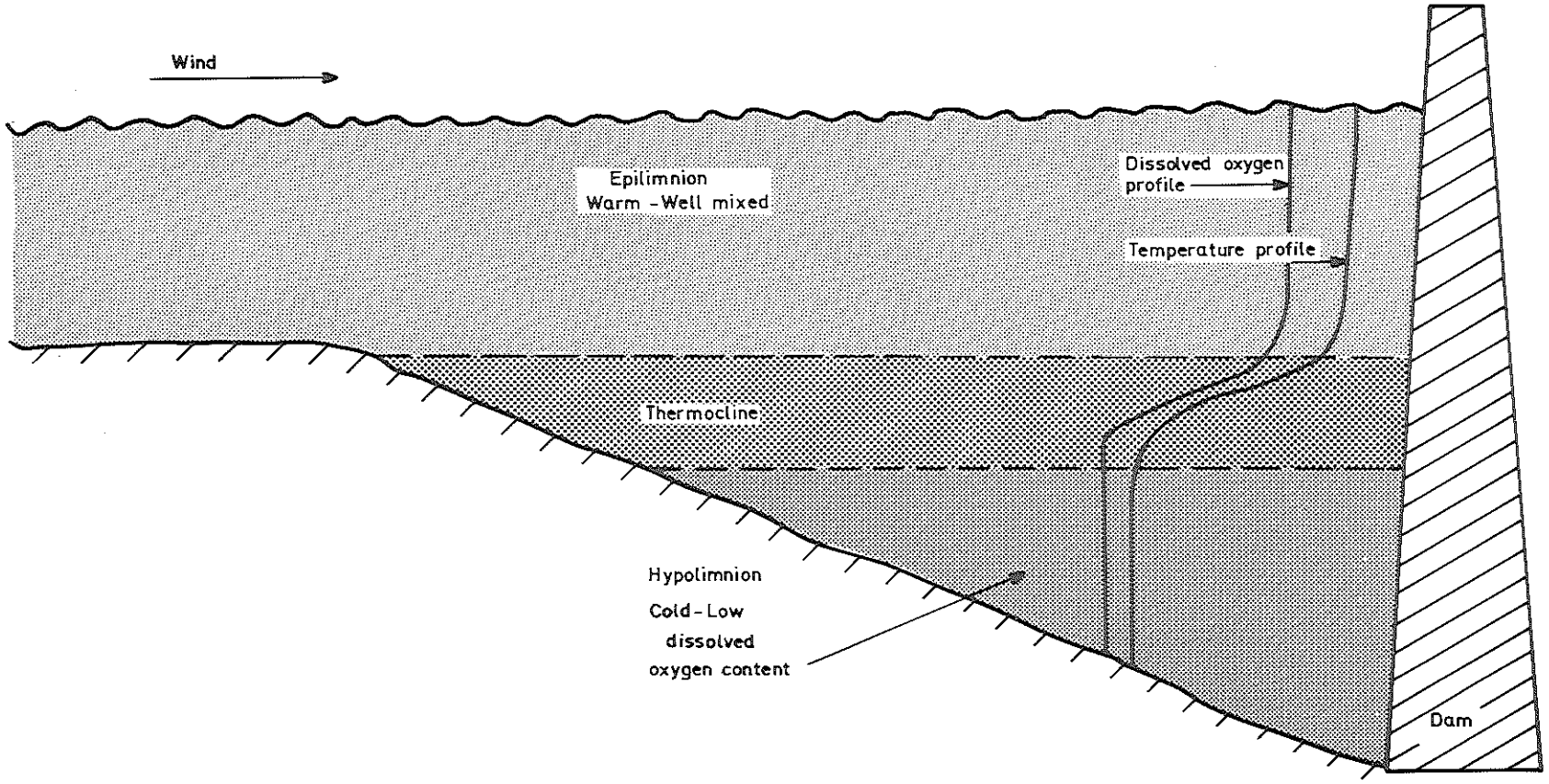

Definition of terms in a stratified impoundment

Fig. 1

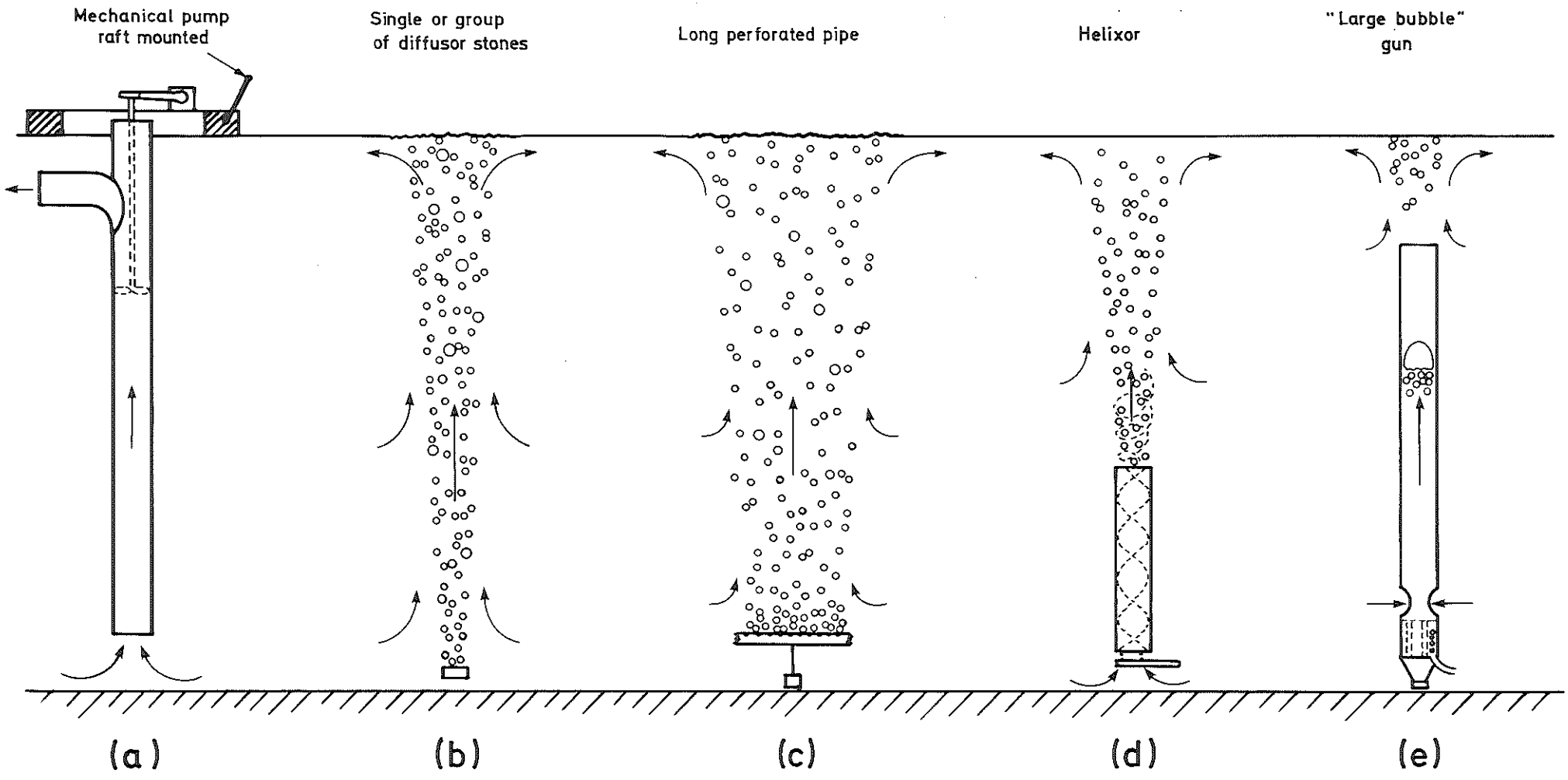

Fig. 2

Methods of artificial destratification

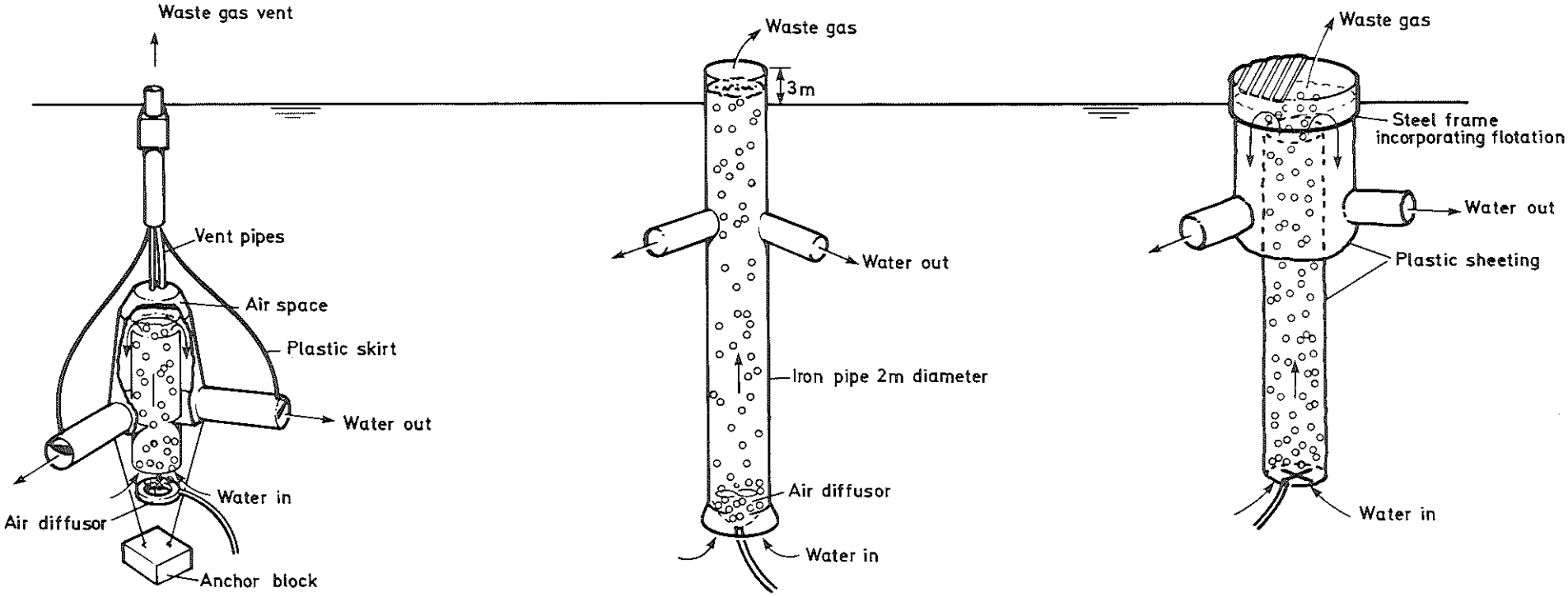

Limno (Atlas Copco)

Wanbach hypolimnion aerator
(Bernhardt reference 8)

Modified full airlift
(proposed by Fast, reference 37)

Fig. 3

Hypolimnion aeration devices

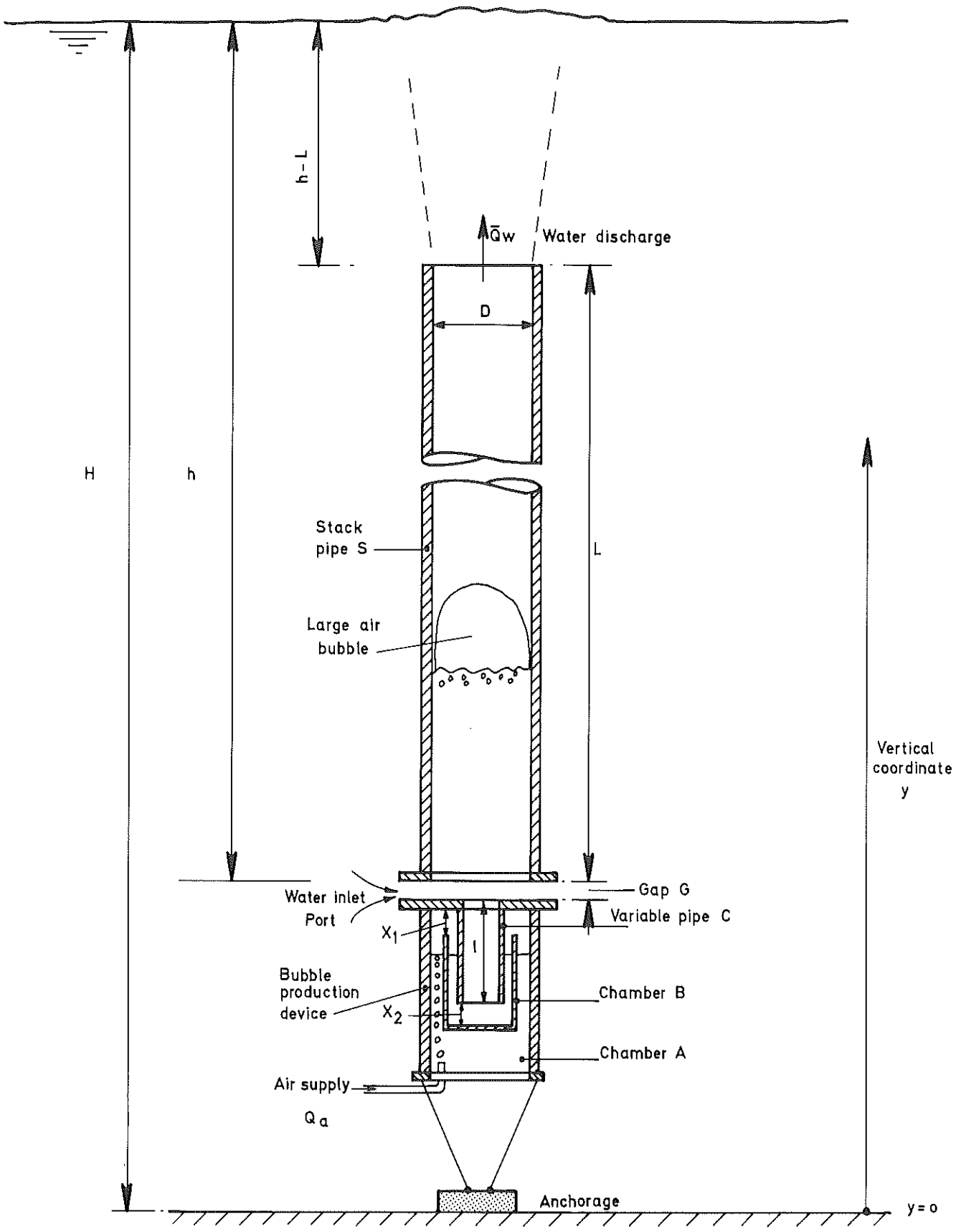

"Large bubble" gun

Fig. 4

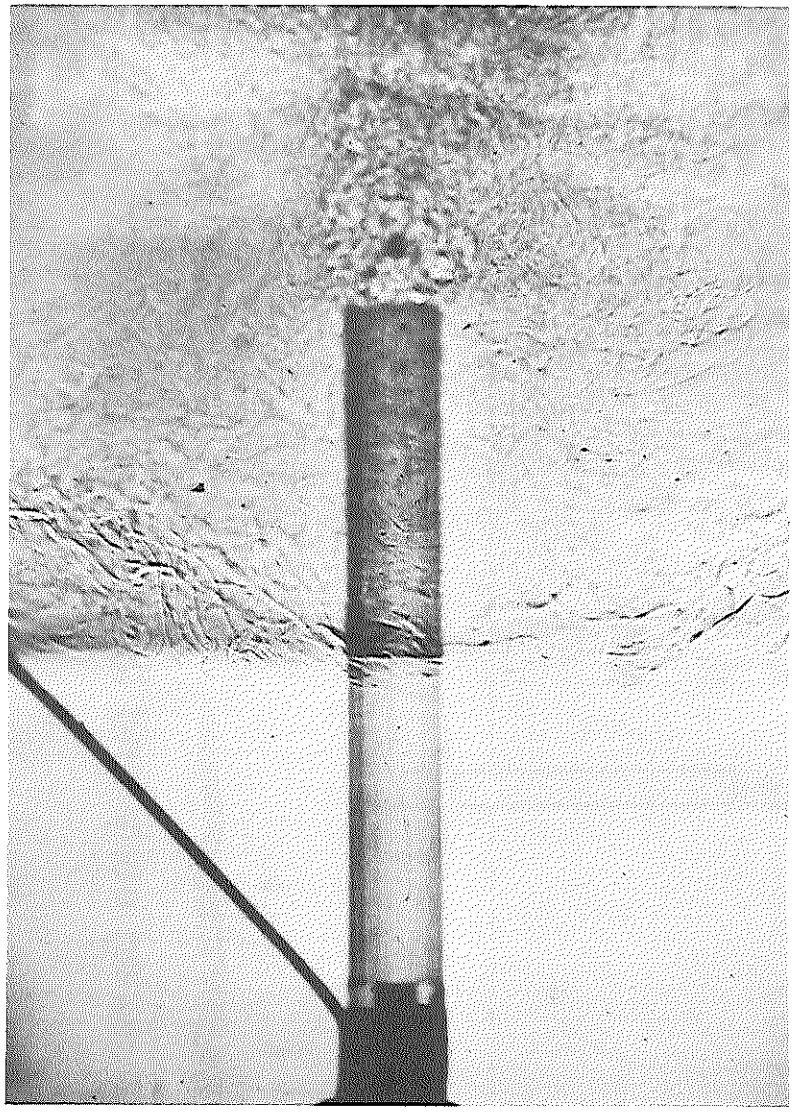

Mixing pattern in the early stage
of the mixing process

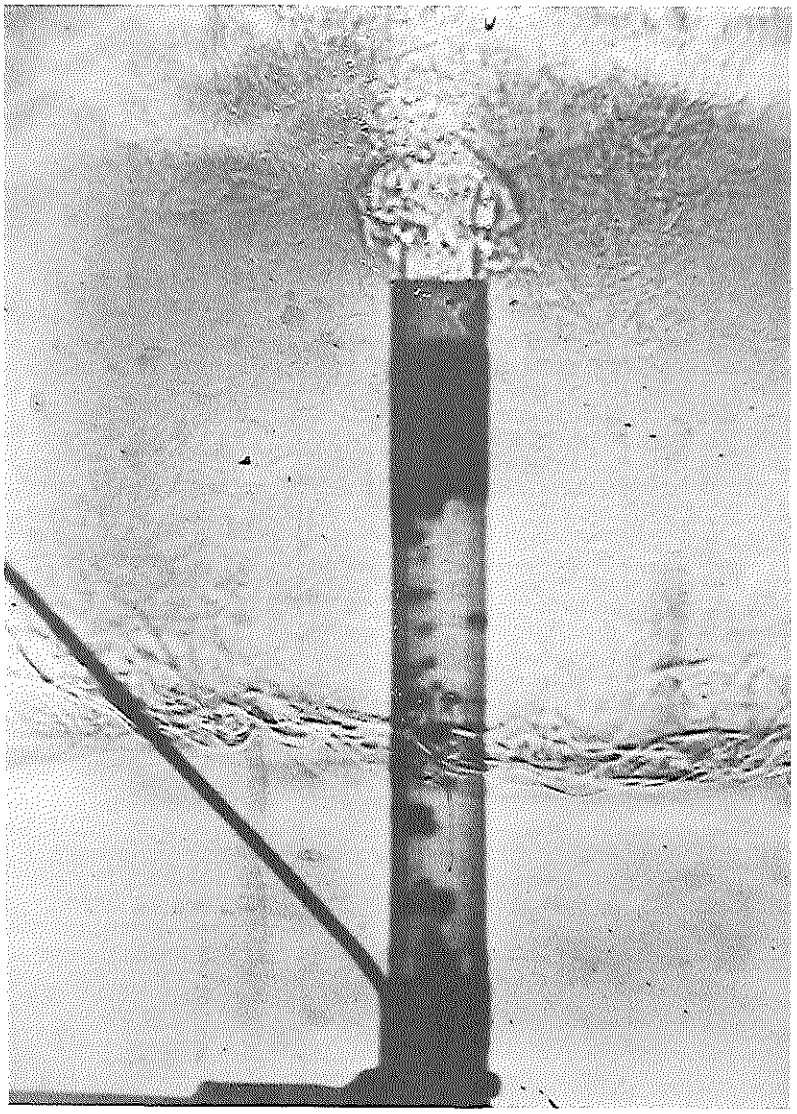

Mixing pattern in the later stage
of the mixing process

Flow visulisation
0·025m dia model Bubble Gun

Fig. 5

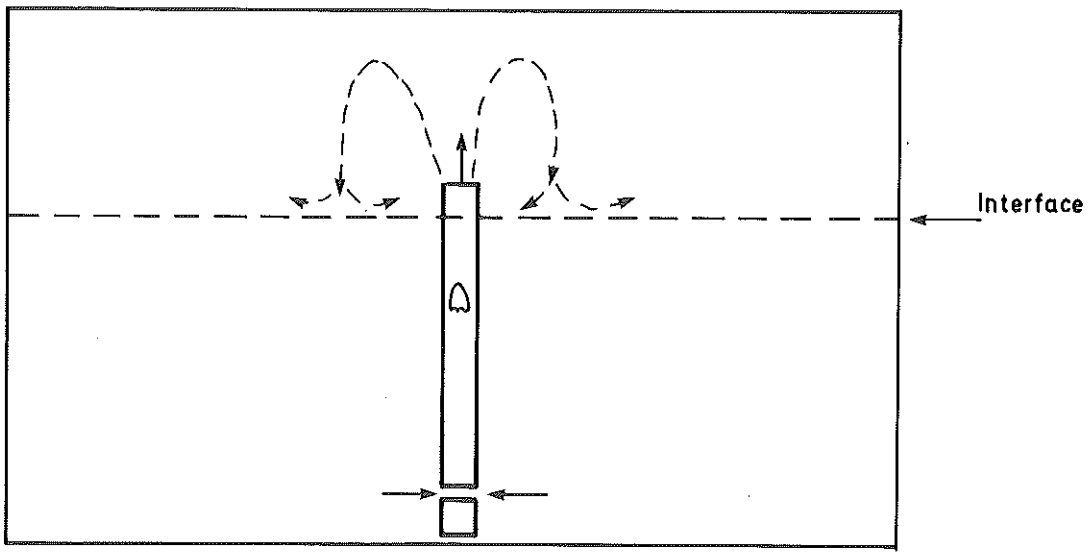

(a) Early stages

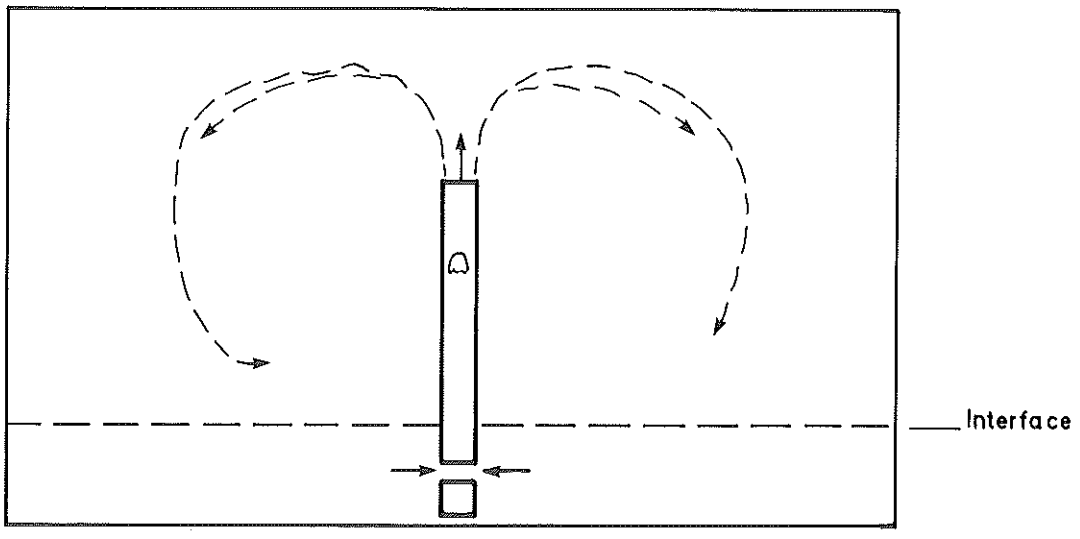

(b) Later stages

Mixing pattern during early and later stage of mixing

Fig. 6

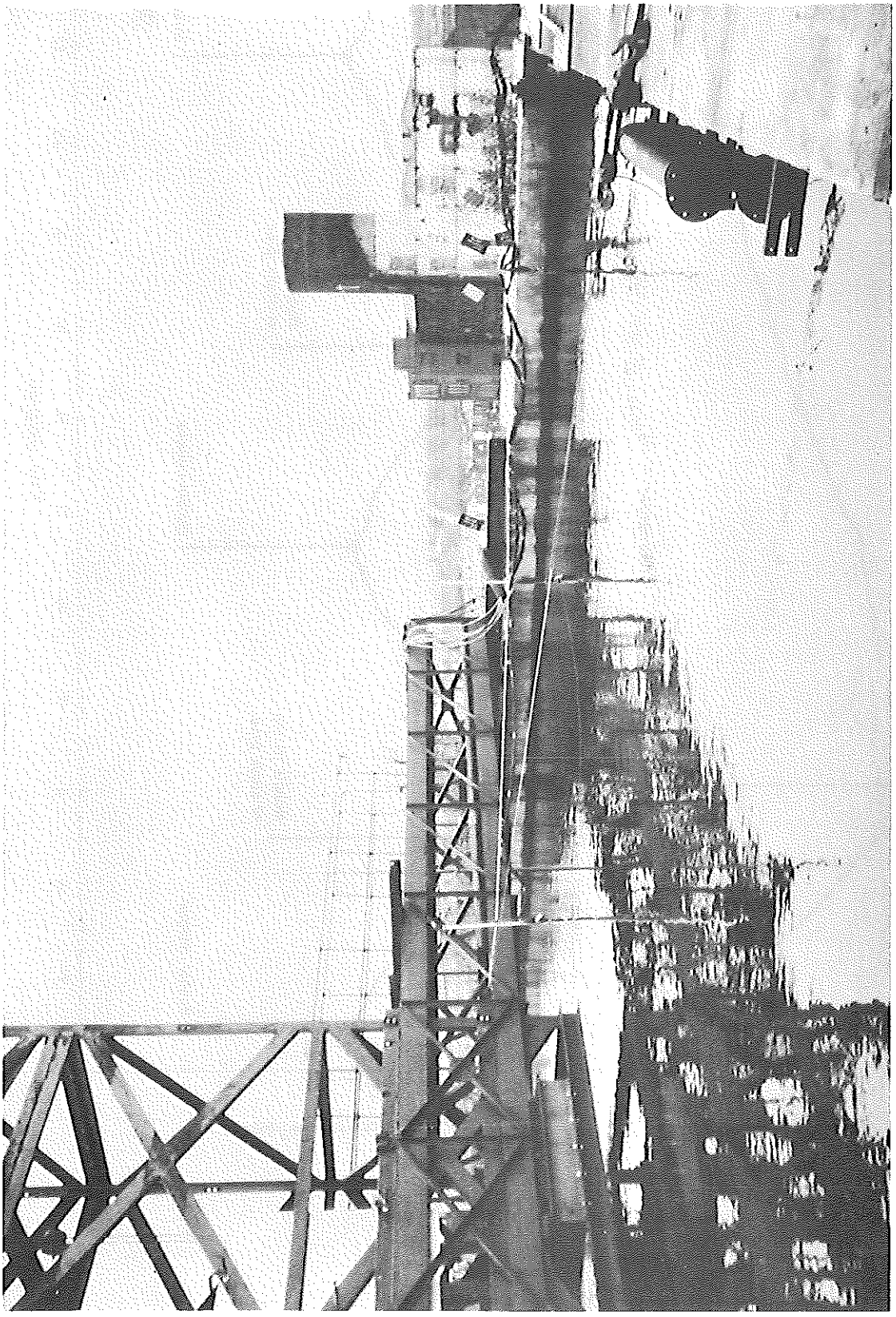

Large test tank

Fig. 7

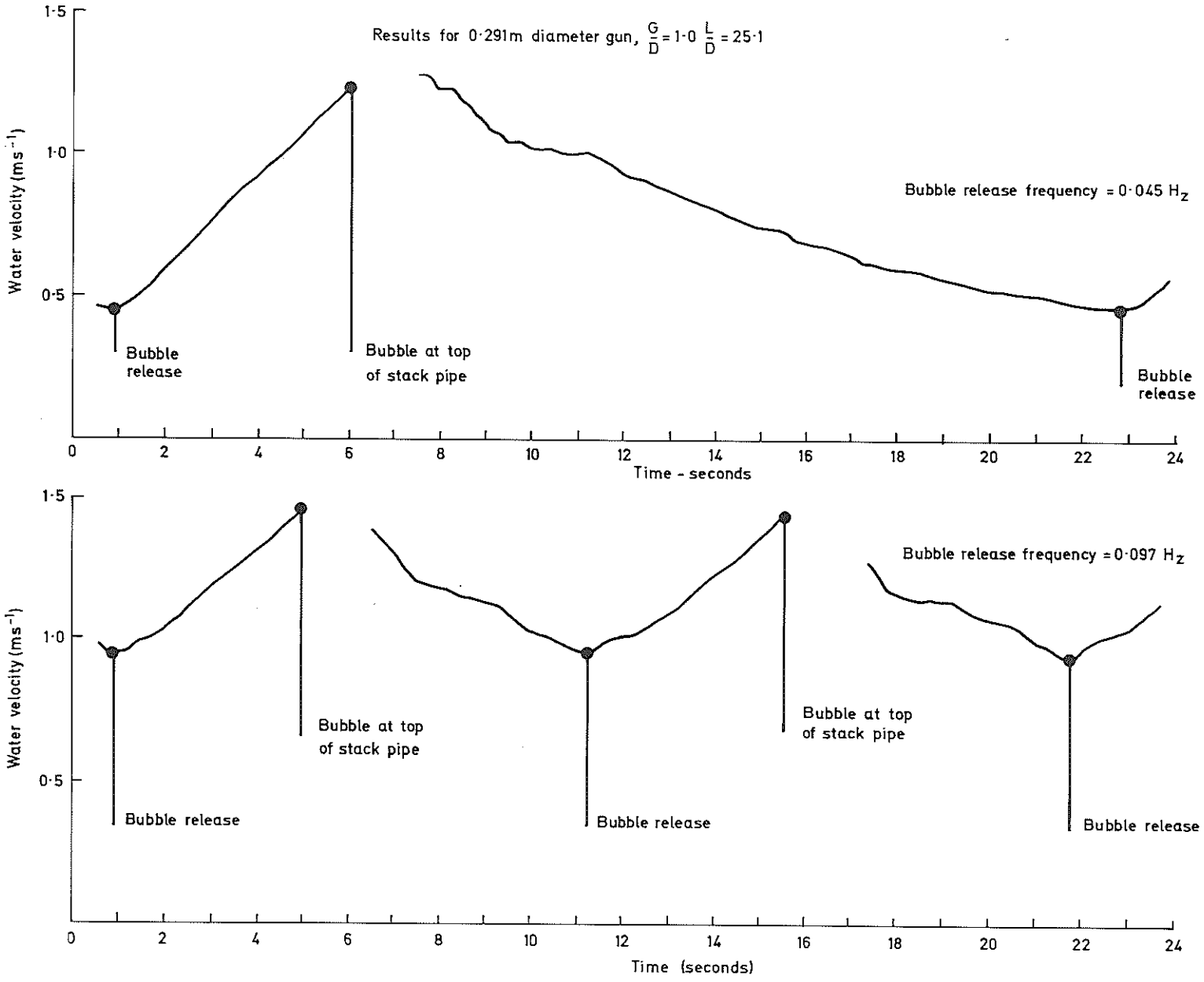

Water velocity at the stack pipe exit as a function of time

Fig. 8

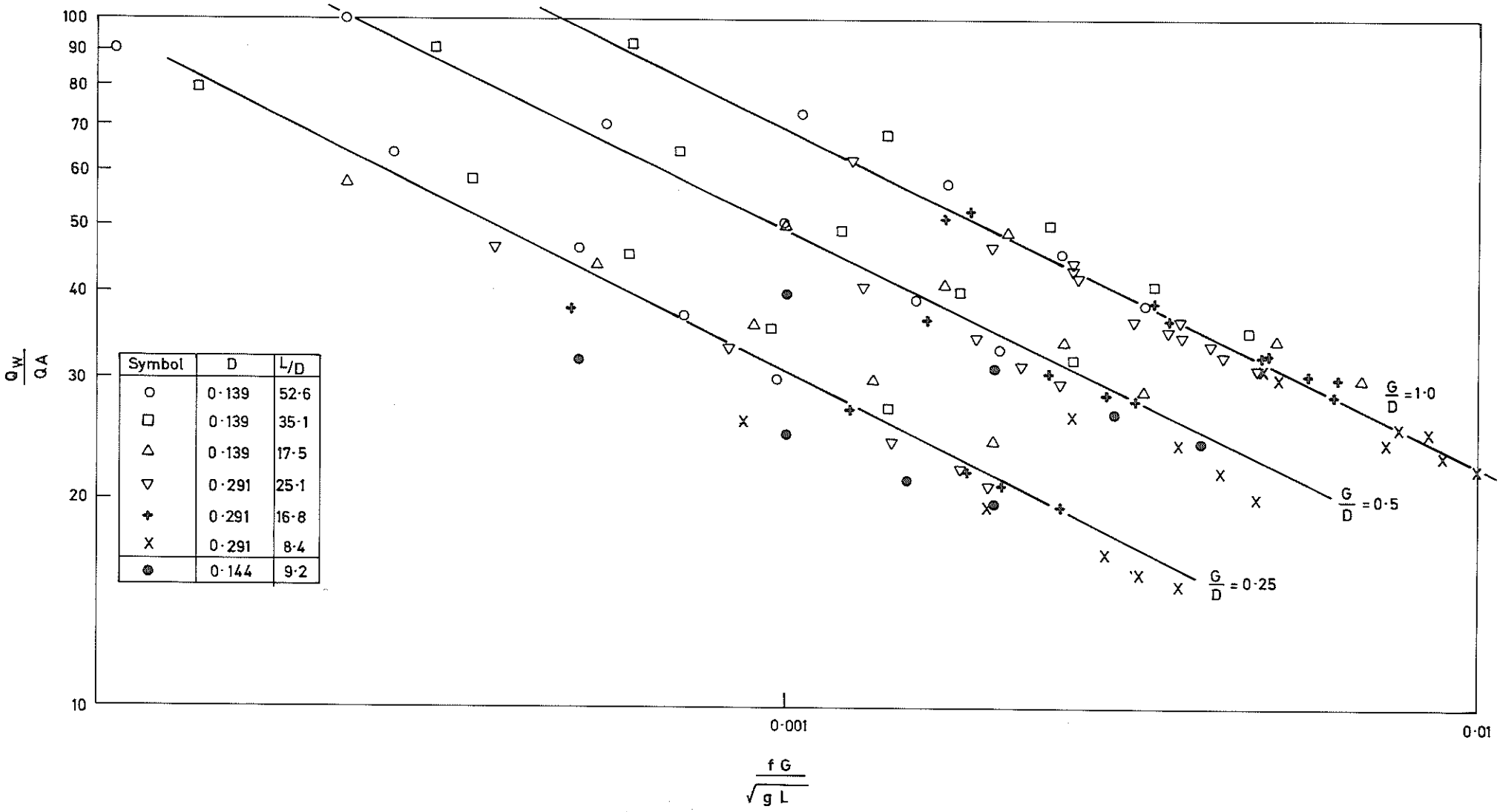

Fig. 9

Pumping performance
of bubble guns

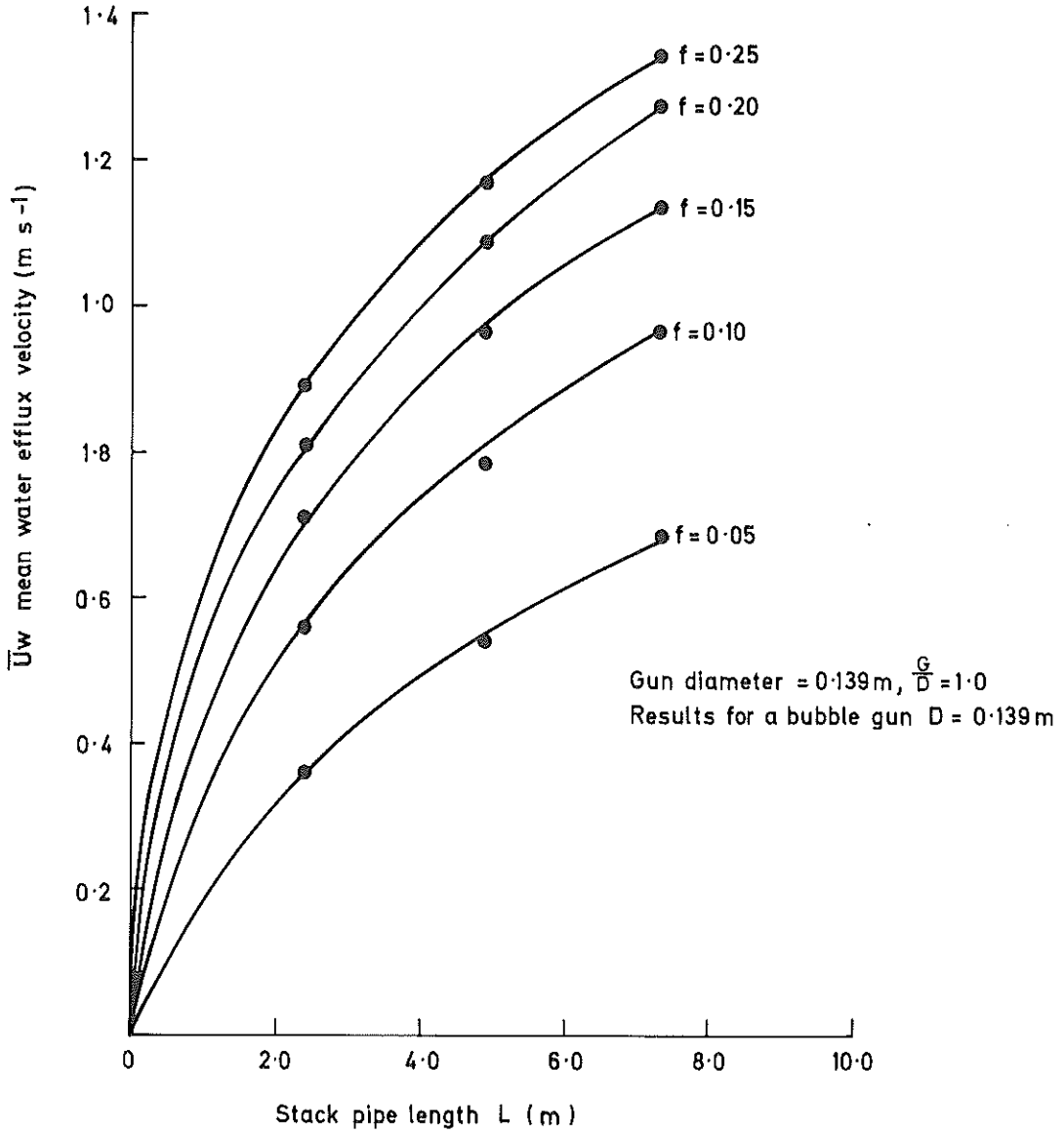

Effect of stack pipe length on mean water velocity

Fig. 10

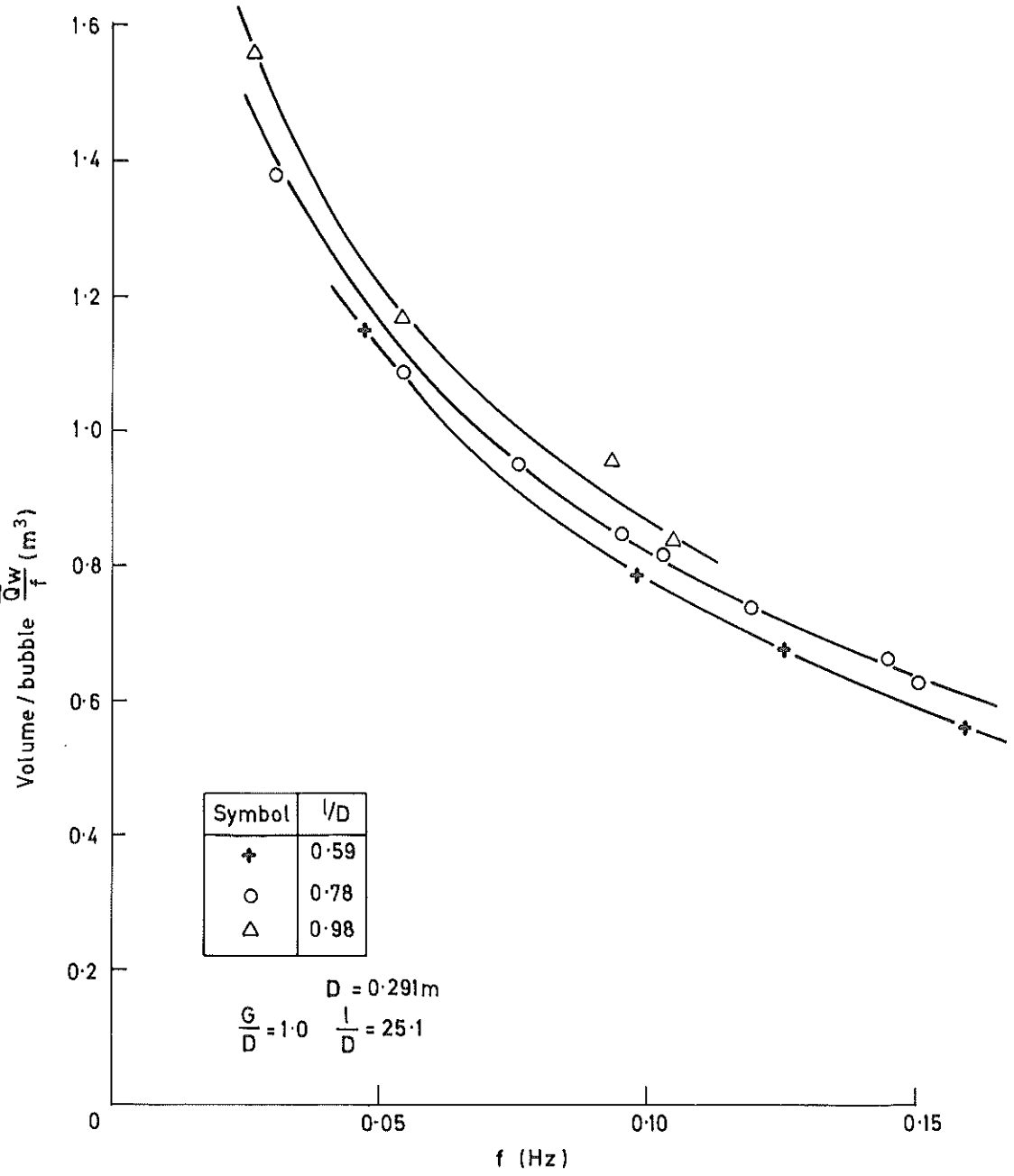

Variation of delivery discharge with bubble frequency

Fig. 11

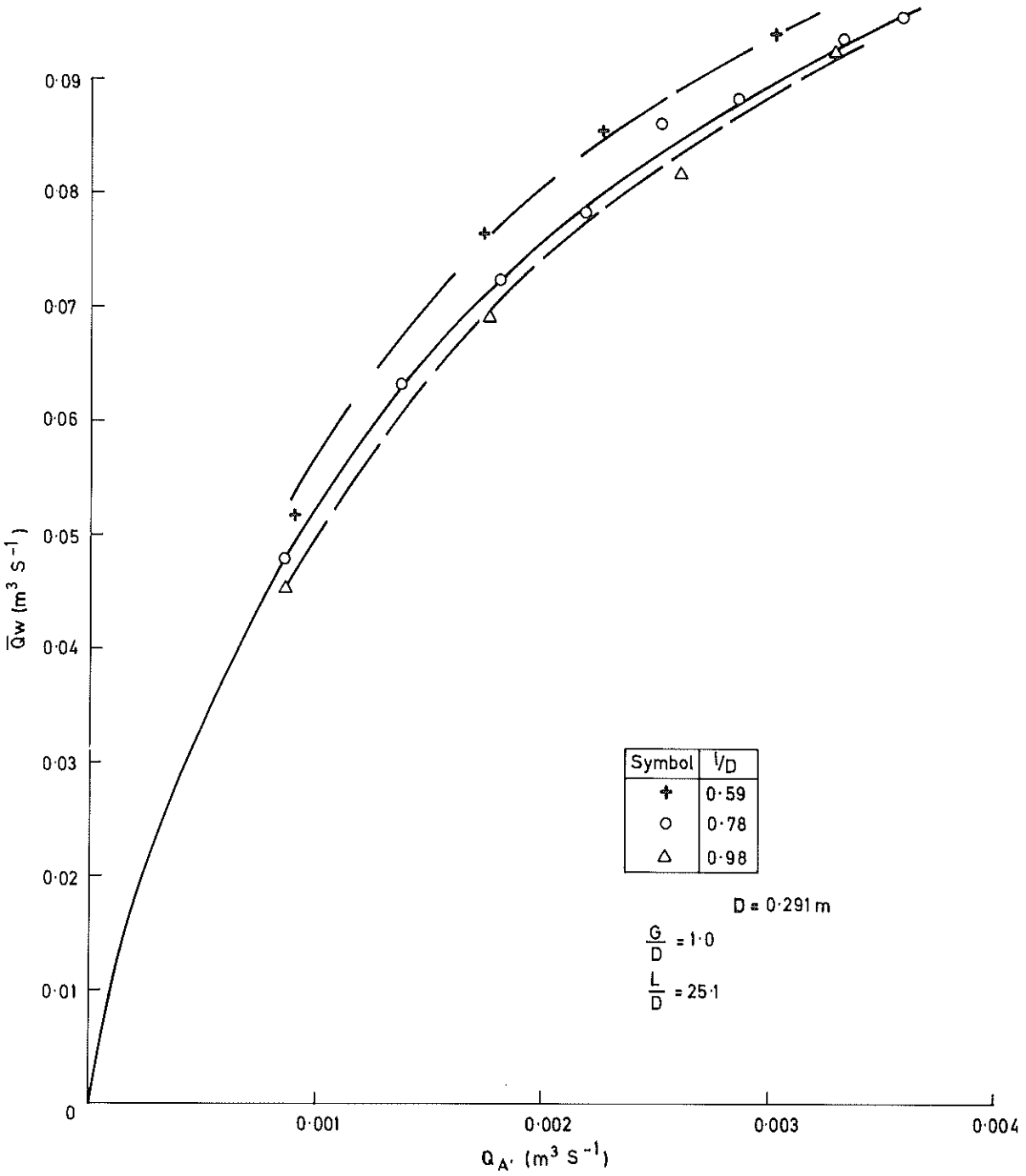

Increase of delivery discharge due to increase of air supply

Fig. 12

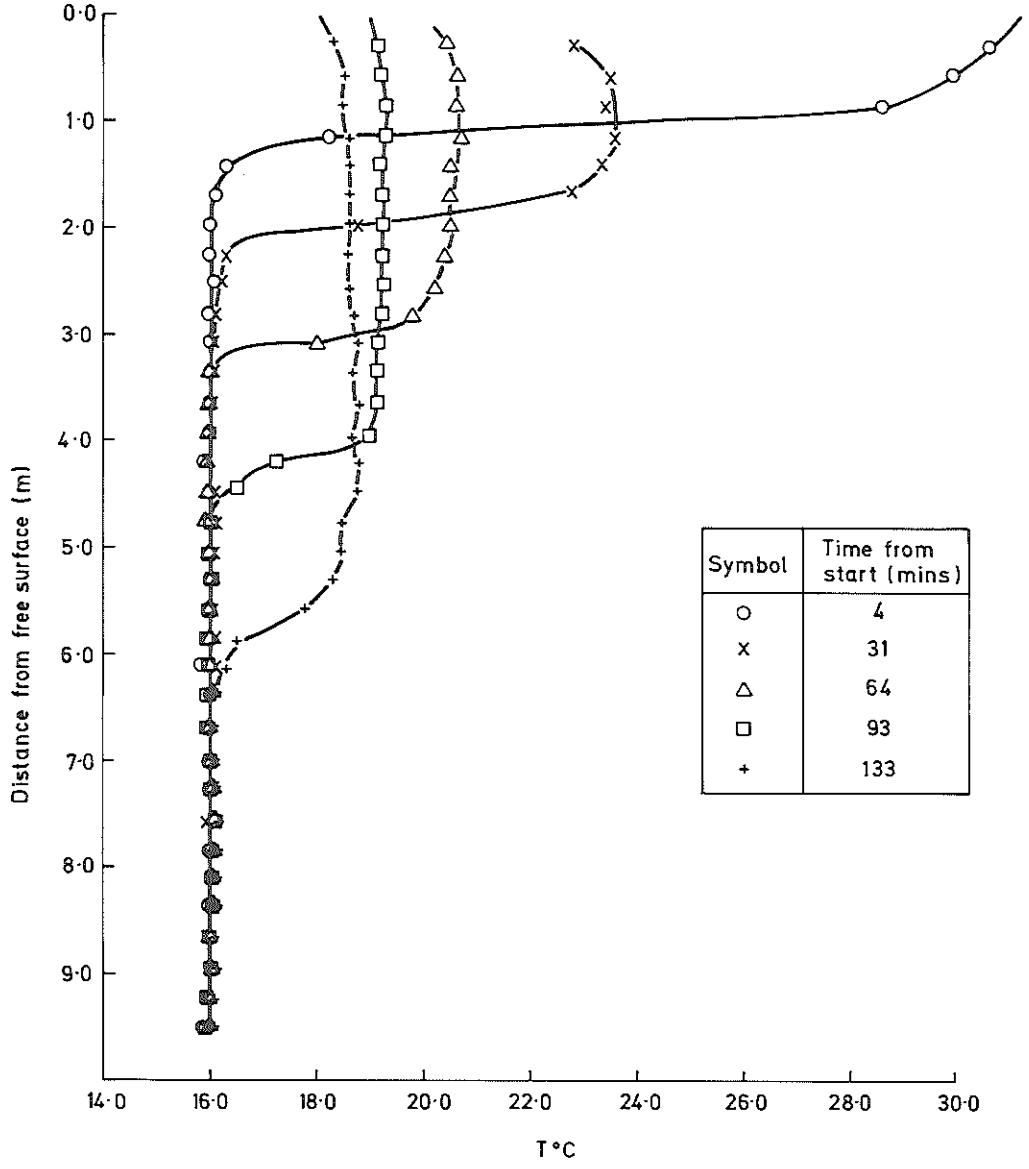

Mean temperature profiles

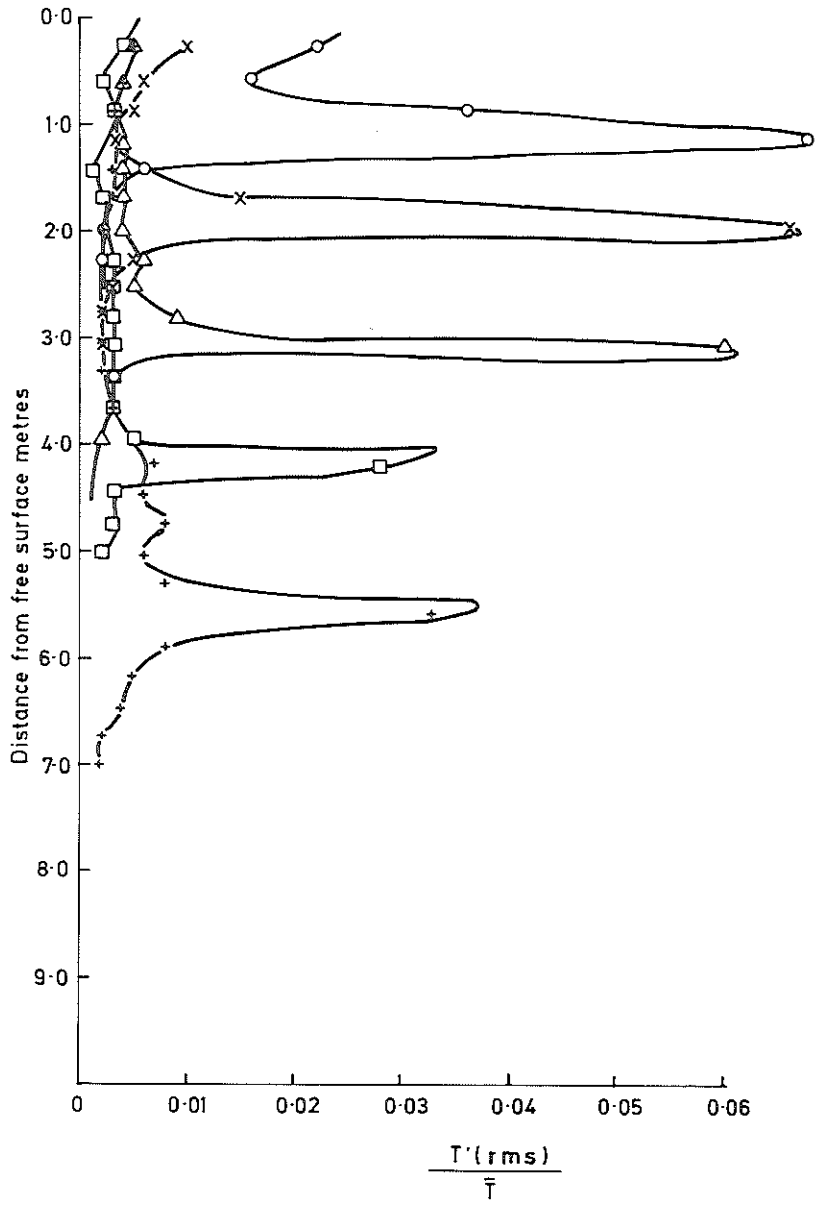

Turbulent intensity profiles of temperature fluctuation

Fig. 13

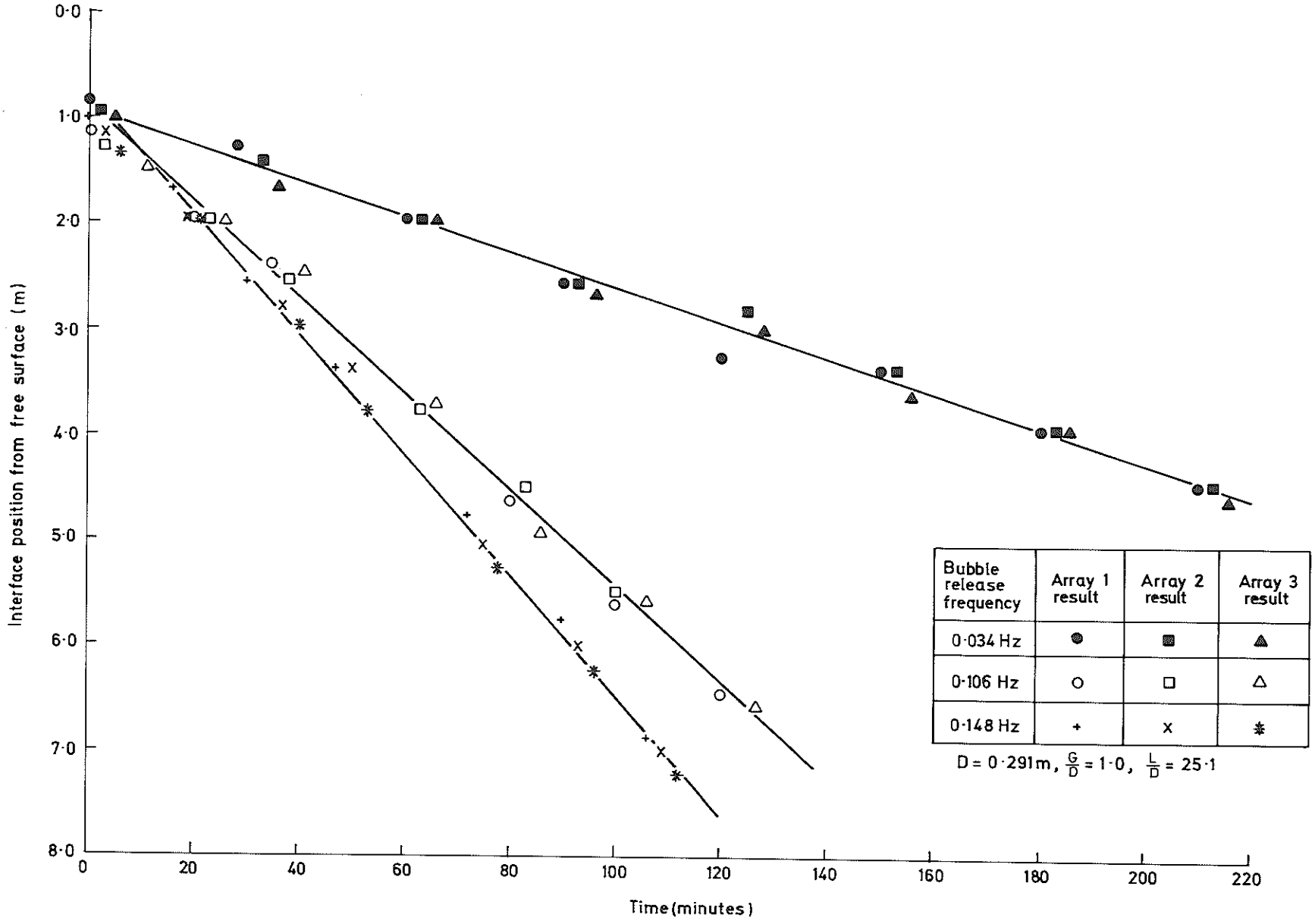

Interface position as a function of time

Fig. 14

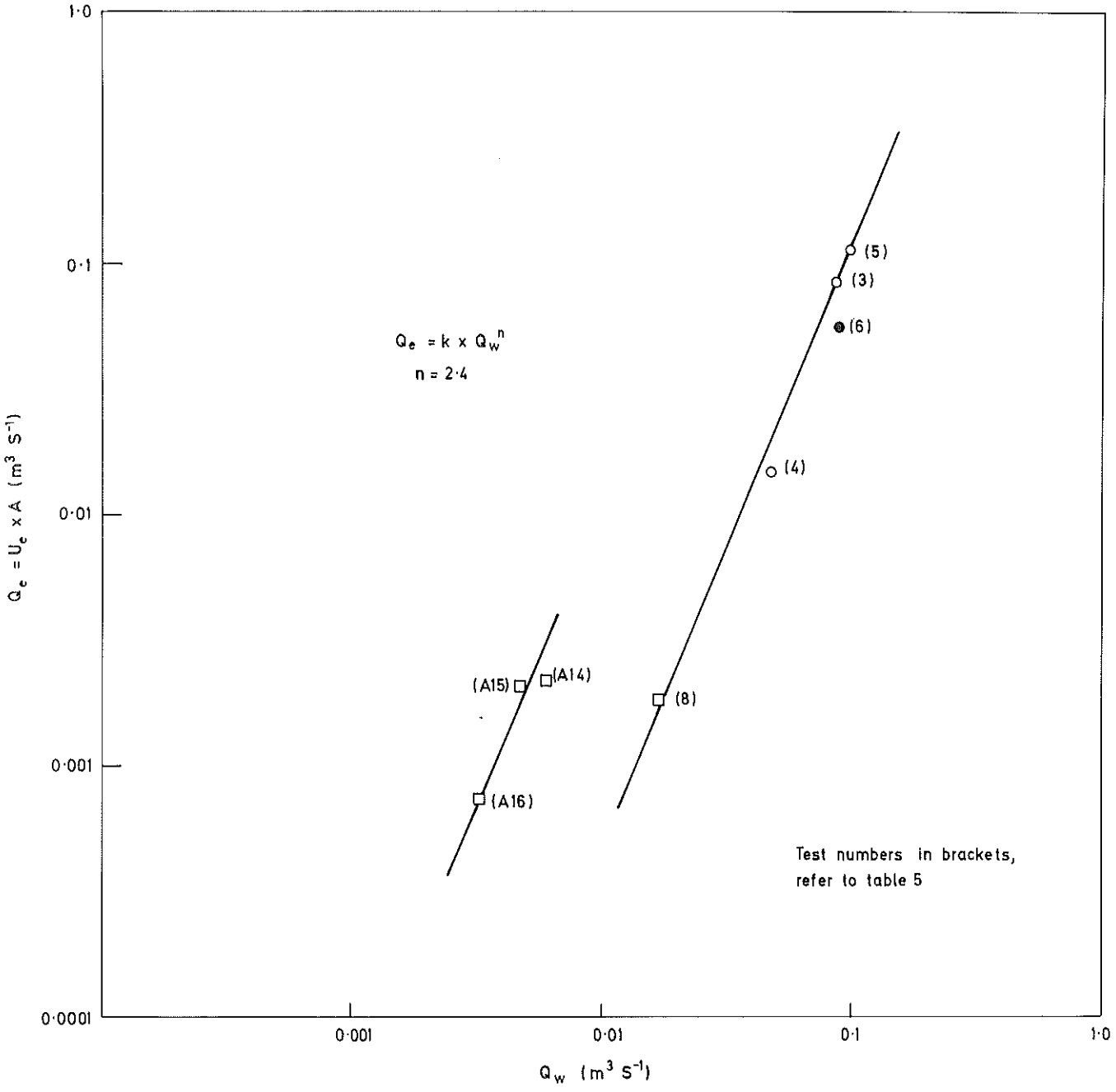

Transfer of water due to induced turbulence in warm water layer

Fig. 15

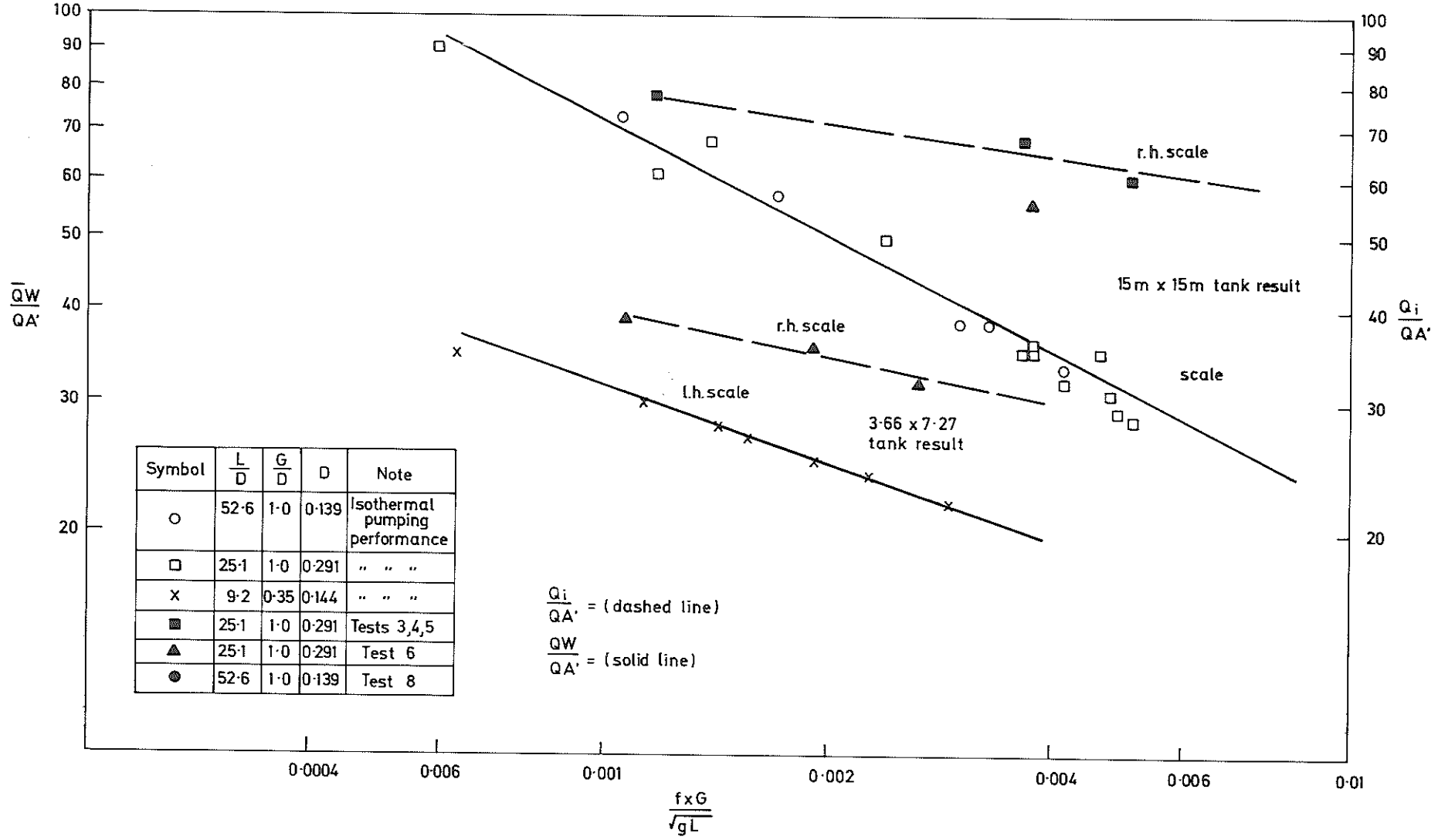

Symbol	$\frac{L}{D}$	$\frac{G}{D}$	D	Note
○	52·6	1·0	0·139	Isothermal pumping performance
□	25·1	1·0	0·291	" " "
×	9·2	0·35	0·144	" " "
■	25·1	1·0	0·291	Tests 3,4,5
▲	25·1	1·0	0·291	Test 6
●	52·6	1·0	0·139	Test 8

Increase of pumping performance due to onset of turbulent entraiment

Fig. 16

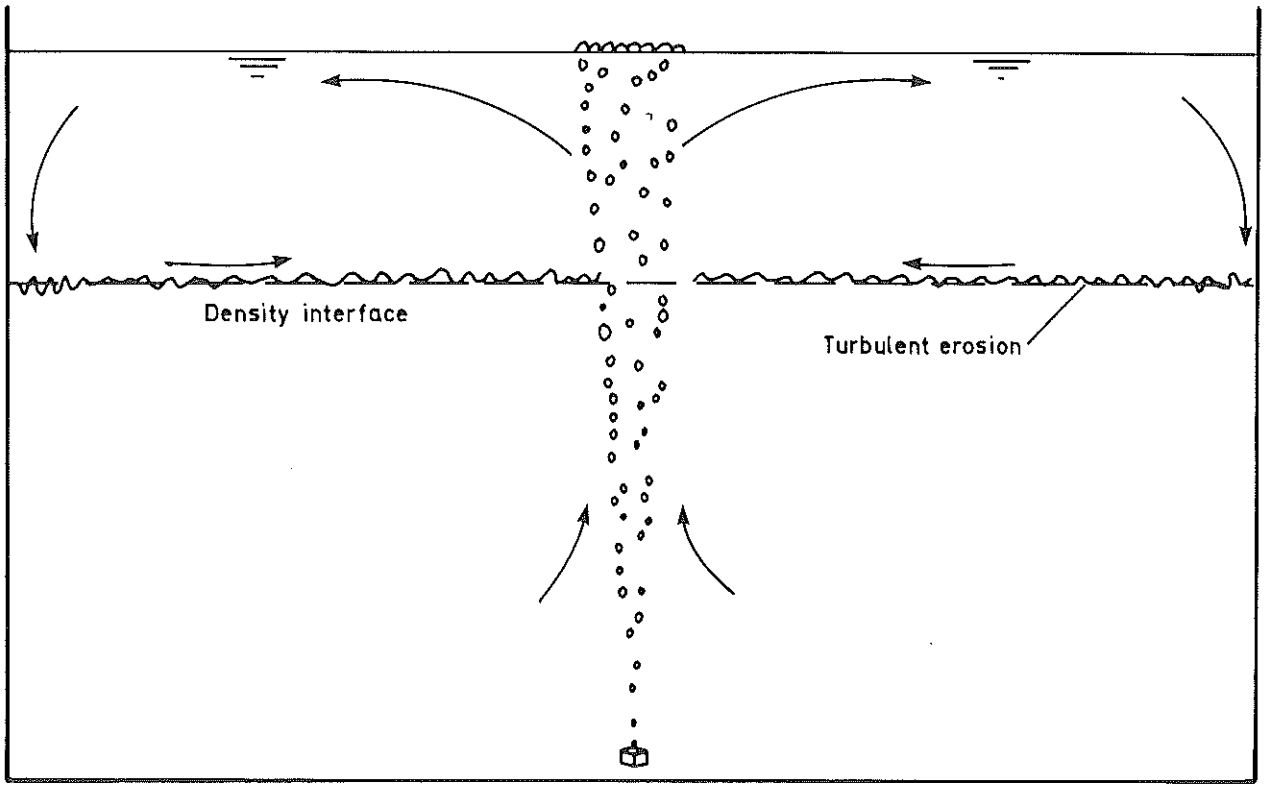

Mixing pattern produced by small air bubble device in a laboratory tank

Fig. 17

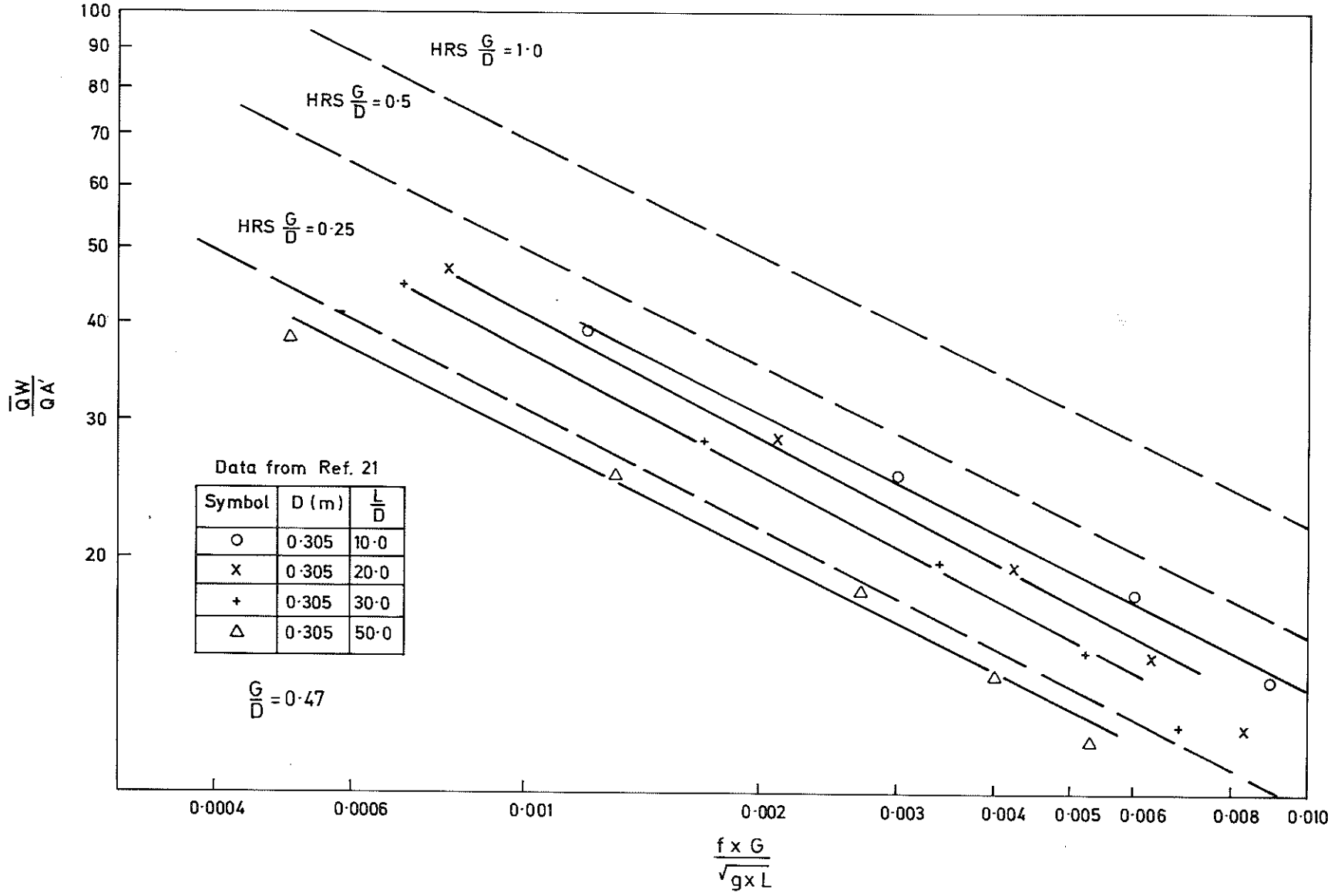

Results of present investigation and those of Ref. 21

Fig. 18

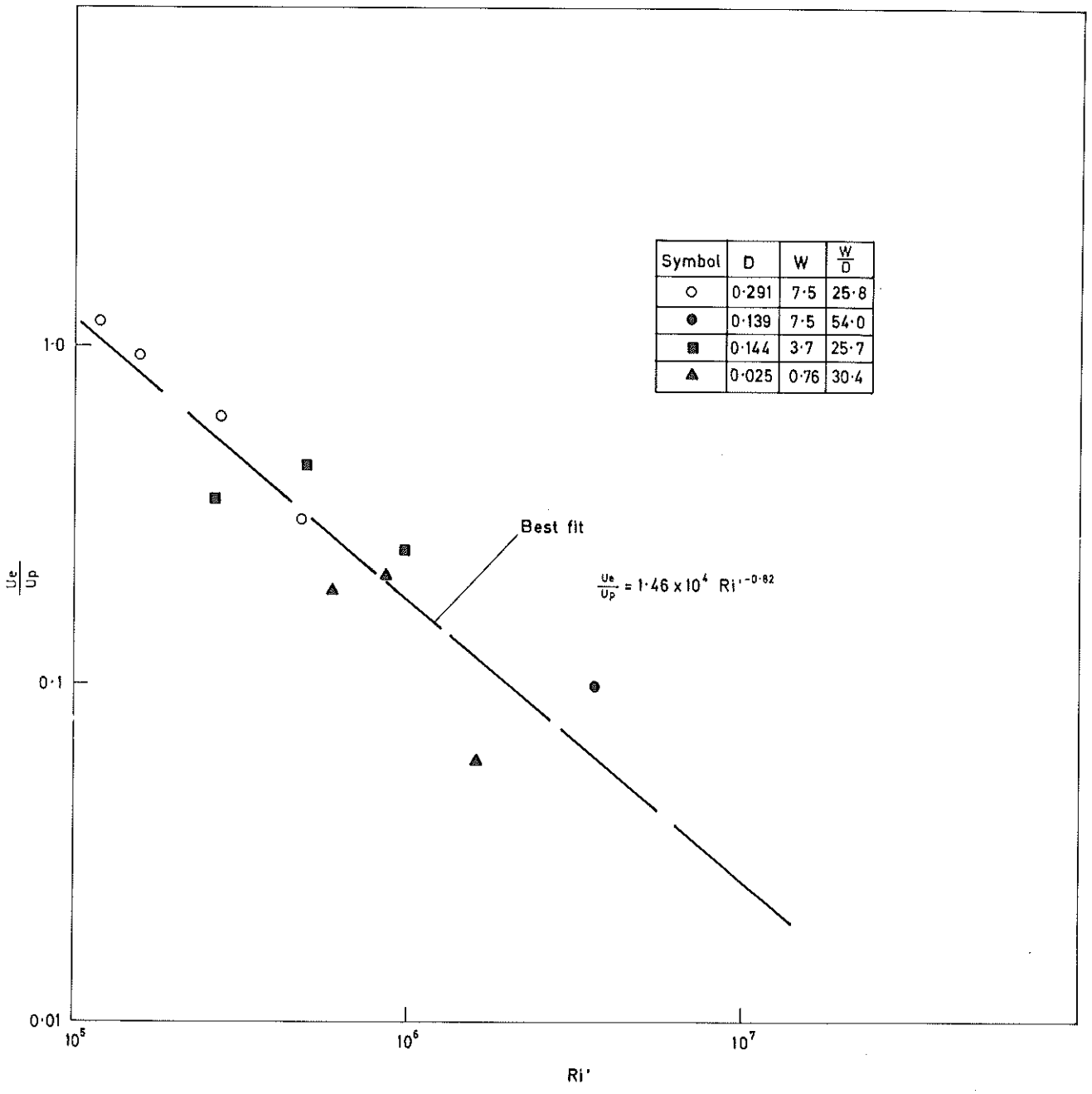

Variation of entraiment velocity with Richardson No. Ri
(Appendix D)

Fig. 19